The Role of MLL1-MENIN Complex in Somatic Cell Reprogramming

by

Alperen YILMAZ

A Dissertation Submitted to the
Graduate School of Sciences and Engineering
in Partial Fulfillment of the Requirements for
the Degree of

Master of Science

in

Molecular Biology and Genetics

July 27, 2023

The Role of MLL1-MENIN Complex In Somatic Cell Reprogramming

Koç University

Graduate School of Sciences and Engineering

This is to certify that I have examined this copy of a master's thesis by

Alperen YILMAZ

and have found that it is complete and satisfactory in all respects,
and that any and all revisions required by the final
examining committee have been made.

Committee Members:

_____

Prof. Tamer Önder

_____

Assoc. Prof. Gözde Korkmaz

_____

Assist. Prof. Nur Mustafaoğlu

Date:_____

ABSTRACT

The role of MLL1-MENIN complex in somatic cell reprogramming

Alperen YILMAZ

Master of Science in Molecular Biology and Genetics

July 27, 2023

Expression of OCT4, SOX2, KLF4 and MYC (OSKM) can reprogram somatic cells to pluripotency. This process involves a complete reset of the somatic cell identity. However, chromatin-based mechanisms that safeguard cellular identities act as barriers to reprogramming, resulting in low efficiency of cell fate conversions. To identify such barriers, a loss of function genetic screen has previously been performed and MLL1 (KMT2A) was identified as a significant roadblock for reprogramming. In the scope of this work, we employed chemical and genetic approaches to characterize the effects of MLL1 in complex with MENIN on reprogramming of human somatic cells. Firstly, we validated the barrier function of this complex via utilizing an inhibitor, VTP50469, that selectively targets MLL1-MENIN complex, which led to increased reprogramming efficiency. Next, we generated fibroblast cell lines that express Cas9 and gRNAs targeting *MLL1* and *MEN1* genes. Reprogramming experiments with these cell lines showed that deletion of both MEN1 and MLL1 increase the efficiency of reprogramming significantly. To further understand the barrier function of this complex, we tested the rescue capabilities different MEN1 point mutants by overexpressing their cDNAs in *MEN1* KO cells. These experiments showed that while MLL1 interaction is crucial for MENIN barrier function, MENIN might be interacting with additional proteins such as JUND to prevent reprogramming. Furthermore, we observed that DOT1L inhibition does not further enhance the reprogramming efficiency when combined with VTP50469 treatment or MEN1 depletion. This suggests that DOT1L-related mechanisms might be involved in the prevention of somatic cell reprogramming. Moreover, we performed RNA-sequencing to identify the transcriptional changes that place in MENIN inhibition and depletion. RNA-sequencing results showed that, compared to the controls, several of pluripotency genes which include genes that are usually expressed in late reprogramming are upregulated both in the context of MENIN inhibition and depletion. In line with that, we observed that a large set of fibroblast-specific genes are downregulated in the absence of MENIN activity. Additionally, we also showed that this complex imposes a barrier function during the resetting of primed pluripotent stem cells to naive pluripotency. The supplementation of the naive culture conditions with VTP50469 enhanced the induction naive pluripotent stem cells. This suggests that MLL1-MENIN inhibition is a feasible target for modulating human naive pluripotency. Taken together, the results represented herein shows that MLL1-MENIN complex imposes barriers in the acquisition of cell identities of higher developmental potential.

ÖZETÇE

Somatik Hücre Yeniden Programlanmasında MLL1-MENİN Kompleksinin Rolü

Alperen YILMAZ

Moleküler Biyoloji ve Genetik, Yüksek Lisans

27 Temmuz 2023

OCT4, SOX2, KLF4 ve MYC (OSKM), ifadesi somatik hücreleri pluripotensiye yeniden programlayabilir. Bu süreç hücre kimliğiyle ile alakalı gen ağının tamamen yeniden düzenlenmesi ile gerçekleşir. Fakat, hücre kimliğini koruyan kromatin-bazlı mekanizmalar yeniden programlamanın düşük verimlilikte olmasına neden olur. Bu tip bariyerleri belirlemek için CRISPR-Cas9 yardımıyla susturma taraması gerçekleştirildi. Bu tarama sonucunda MLL1 yeniden programlamayı engelleyen güçlü bir bariyer olarak ortaya çıktı. Bu çalışma kapsamında, kimyasal ve genetik yaklaşımlar ile MLL1'in MENIN proteiniyle oluşturduğu kompleksin bariyer özelliği karakterize edildi . İlk olarak MLL1-MENIN kompleksin yeniden programlamaya bariyer özelliği gösterdiğini doğrulamak için bu kompleksi hedefleyen bir inhibitörü, VTP50469, kullanarak yeniden programlama veriminin arttığını doğrulandı. Sonrasında CRISPR-Cas9 yardımıyla MEN1 ve MLL1 genleri susturulmuş hücre hatları oluşturuldu. Oluşturulan bu hücre hatlarıyla yapılan yeniden programlama deneyleriyle MLL1 ve MENIN proteinlerinin ikisinin de yeniden programlama verimini arttırdığı gözlemlendi. Bu kompleksin bariyer özelliğini daha iyi anlayabilmek için MEN1 geni susturulmuş hücrelerde farklı nokta mutasyonları ifade ettirilmiştirdi. Bu hücrelerle yapılan yeniden programlama deneyleri MENIN ve MLL1 etkileşiminin MENIN'in bariyer fonksiyonu için oldukça önemli olduğunu göstermeye ek olarak, MENIN proteinin JUND gibi başka proteinlerle de etkileşime girerek somatik hücre yeniden programlanmasına engelliyor olabileceğine işaret etti. Ayrıca, MENIN inhibisyonunda ve susturulmasında gerçekleşen transkripsiyonel değişiklikleri belirlemek için RNA sekanslaması gerçekleştirdik. RNA sekanslama sonuçları aralarında geç yeniden programlama evrelerinde ifade edilmeye başlayan genleri de içeren pluripotensi ile alakalı genlerin MENIN inhibisyonunda ve susturulmasında daha fazla ifade edildiğini gösterdi. Bununla uyumlu bir şekilde, MENIN aktivitesi olmadığında fibroblast kimliği ile alakalı geniş bir gen setinin de ifadesinin azaldğını gösterdik. Ek olarak, DOT1L inhibisyonunun VTP50469 uygulamasıyla veya MEN1 susturulmasıyla ilave bir etkisinin olmadığı gözlemlendi. Son olarak, bu kompleksin aynı zamanda konvansiyonel "primed" kök hücrelerin naif pluripotensiye dönüştürülmesinde de bariyer özelliği gösterdiği tespit edilmiştir. Naif hücre ortamına VTP50469 eklenmesi naive kök hücre eldesini daha güçlü hale getirmiştir. Bu durum MLL1-MENIN kompleksinin insan naif pluripotensisini modüle etmek etmek için uygun bir hedef olduğunu göstermektedir. Hepsi birden düşünüldüğünde, MLL1-MENIN kompleksinin daha yüksek gelişimsel potansiyelli hücre kimliklerinin kazanılmasında bariyer oluşturduğu gösterilmiştir.

ACKNOWLEDGEMENTS

I would like to thank my advisor, Prof. Tamer Önder, for all of his guidance during my training in his laboratory. In addition to learning how to approach scientific questions, I learned how to acquire and present data of high quality.

I am very thankful to have Dr. Gülben Gürhan as my labmate. We have learned a lot in the lab together. Working with her, especially during difficult times, has been a relief I didn't know I needed. I hope to continue working on bigger and more ambitious projects with her in the coming years.

I would also like to thank Şevval Nur Bektaş. I feel thankful to have mentored her as my intern in the lab. Her work was crucial for this project. I have high hopes that she will be successful in anything she decides to do with her life.

I would like to thank Cathy Lee and Charles Henry Gierke. They are the reasons why I am who I am today. Unfortunately, last year, Charles passed away. Despite our disagreements from time to time with him, I have always known that he had a kind heart full of love. I will always cherish the lessons I learned from both of them.

I would like to thank Birol Yıldız. His support came at a time I needed the most. This endeavor would not be possible without his support.

I would like to thank my family for supporting me during my training.

Lastly, I would like to thank Elifsu Polatlı for being such a supportive and patient girlfriend with a workaholic boyfriend. Her support was crucial in navigating through my Master's degree.

TABLE OF CONTENTS

LIST OF TABLES

LIST OF FIGURES

ABBREVIATIONS

ESC	Embryonic Stem Cell
PSC	Pluripotent Stem Cell
TGFB	Transforming Growth Factor Beta
ROCK	Rho-associated Kinase
LIF	Leukemia Inhibitory Factor
VPA	Valproic Acid
NaBut	Sodium Butyrate
HENSM	Human Enhanced Naive Stem Cell Medium
MEF	Mouse Embryonic Fibroblasts
OCT4	Octamer-binding Transcription Factor 4
SOX2	SRY-box Transcription Factor 2
KLF4	Krüppel-like Factor 4
iPSC	Induced Pluripotent Stem Cell
ADAM	A Disintegrin and Metalloproteinase
OSKM	Oct4, Sox2, Klf4, cMyc
DMSO	Dimethyl Sulfoxide
SAHA	Suberylanilide Hydroxamic Acid
TSA	Trichostatin A
HOX	Homeobox
DMEM	Dulbecco's Modified Eagle Medium
PBS	Phosphate Buffered Saline
KO	Knock-out
RT-qPCR	Real Time Quantitative Polymerase Chain Reaction
cDNA	Complementary DNA
HDAC	Histone Deacetylase
MEN1	Multiple Endocrine Neoplasia 1
MLL1	Mixed Lineage Leukemia 1

Chapter 1:
INTRODUCTION

1.1 Embryonic development and embryonic stem cells

Embryonic development starts with the fertilization of the egg by the sperm. Soon thereafter, cells start to divide and move through subsequent stages of development. After the morula stage, a blastocyst is formed which consists of 3 lineages involving epiblast, trophoblast and hypoblast. While the extraembryonic tissues are formed from the trophoblast and the hypoblast, the epiblast cells presiding in the inner cavity of the blastocyst form the embryo proper which later gives rise to all of the tissues found in the adult organism (Leung & Zernicka-Goetz, 2015). Embryonic stem cells (ESCs) which are derived from the epiblast cells at the blastocyst stage possess a unique capability called "pluripotency", which means that these cells can differentiate into three founding germ layers of embryonic development, mesoderm, endoderm and ectoderm. This state of high potential provides vast possibilities in modeling disease and development in addition to the capability of generating lost or damaged tissues in the context of regenerative medicine (Zernicka-Goetz & Hadjantonakis, 2014).

The use of ESCs in research and therapy have been limited due to the several drawbacks stemming from the derivation methods of these cells which include destruction of human blastocysts. The ethical issues that are raised in the acquisition of these cells have hampered the efforts to utilize these cells in research and development. In fact, the derivation of embryonic stem cells is illegal in many countries (Lo & Parham, 2009). In addition to the ethical issues, it has also proven difficult to obtain embryonic stem cells that would not cause immune reactions in the case that the differentiated cells are implanted (Swijnenburg et al., 2008). To circumvent these issues, defining approaches to acquire pluripotent stem cells has been investigated (Takahashi & Yamanaka, 2006).

1.2 Different states of pluripotency

During the blastocyst stage, the pluripotent cells (PSCs) that form the epiblast possess unique capabilities that distinguish them from the pluripotent cells that are present after the implantation of the embryo to the uterus. These two populations of cells are called naive and primed pluripotent stem cells to distinguish the pre- and post-implantation epiblast, respectively. Unlike the primed PSCs, naive PSCs are not dependent on MEK/ERK pathway activity, have an active X chromosome and exhibit DNA hypomethylation. Moreover, the general pluripotency marker OCT4 is expressed via different enhancer elements in these different pluripotency states. Naive PSCs express OCT4 via the distal enhancer element while primed PSCs express OCT4 via its proximal enhancer element. The latter factor has been utilized in developing reporters to distinguish the different pluripotent states (Theunissen et al., 2014). Additionally, naive cells have a distinctive packed dome-shaped morphology unlike the primed cells having a flat shape (Bayerl et al., 2021).

Two populations of PSCs differ in terms of their differentiation potential as well. While primed PSCs can give rise to all of the tissues of the embryo proper, the naive PSCs have a much greater plasticity to form the extraembryonic tissues as well. This plasticity makes them a viable resource for modeling the early human embryo development, which is inaccessible due to the ethical issues. In 2022, Kagawa et al. showed that when naive cells are aggregated under special media conditions (MEK/ERK inhibition, TGFB inhibition, ROCK inhibition and Hippo inhibition), they form structures that resemble days post fertilization (dpf) 5-7 blastocysts with three founding lineages: trophectoderm, primitive endoderm and epiblast. These “blastoids” resemble the in vivo blastocysts both transcriptionally and morphologically (Kagawa et al., 2022). Another study that highlighted the importance of naive cells in modeling embryo development came in 2022. Tarazi et al. showed that mouse naive cells can create post-gastrulation mouse embryo-like structures without any sperm, egg or uterus. In their work, they showed that by aggregating naive cells that were overexpressing the necessary lineage genes for extraembryonic tissue with the naive cells without any overexpression leads to the self-organization of the tissue to become a bona fide post-gastrulation embryo (Tarazi et al., 2022). While this work required the use of exogenous transgenes to instruct the cells to acquire extraembryonic lineage identities, it has been shown that human naive PSCs do

not require them. In fact, in 2023, Oldak et al. showed that it is possible to generate Carnegie stage 6a human embryo models that were derived from human naive pluripotent stem cells without the use of any exogenous transgenes (Oldak et al., 2023). This latest human embryo model highlighted the fact that human naive pluripotent stem cells are key in understanding early human development which has been very difficult to study previously due to ethical issues.

Traditionally, mouse ESCs and human ESCs differ in terms of their developmental potential. While mESCs grown in 2i (PD0325901 and CHIR99021) + LIF condition possess the characteristics of the naive state, conventional human ESCs resemble the post-implantation epiblast-like primed state (Takashima et al., 2014). While the culture conditions for the naive state for rodents have been well established, the culture conditions for establishing and maintaining this naive state for human were not described until recently. One of the key studies that described the acquisition of the naive state came from the laboratory of Austin Smith where, they reported that it is possible to "reset" the human primed cells to become naive cells via the overexpression of NANOG and KLF2 genes (Takashima et al., 2014). Using a DOX inducible system, they showed that reset naive cells can be maintained and expanded with 2iL media that is used for culturing mESCs in the presence of DOX. They also defined additional components to stabilize the acquired naive identity without overexpressing NANOG and KLF2 (Takashima et al., 2014). In 2019, the same group defined the conditions necessary for acquiring naive cells without the use of transgenes. This method utilized broad histone deacetylase (HDAC) inhibitors such as valproic acid (VPA) and sodium butyrate (NaBut) for the initial acquisition of naive pluripotency and PXGL (PD0325901 (MEK-ERK inhibitor), XAV939 (WNT inhibitor), 2 μM Gö6983 (Protein Kinase C inhibitor) and 10 ng/mL human LIF (JAK-STAT activator)) media for the stabilization and maintenance of the naive PSCs (G. Guo et al., 2017). In 2021, Jacob Hanna and colleagues described a slightly different approach of acquiring human naive pluripotent stem cells (Bayerl et al., 2021). In their paper, they utilized a reporter human ESC cell line (Theunissen et al., 2014) that was genetically modified to give GFP signal when the cells start to express the OCT4 gene via the distal enhancer element, which is a hallmark characteristic of naive pluripotency. They identified a cocktail of compounds and cytokines that enables the acquisition and maintenance of the naive pluripotent cells. This cocktail of inhibitors, named Human Enhanced Naive Stem Cell medium (HENSM) included PD0325901

(MEK-ERK inhibitor) , XAV939 (WNT inhibitor), Gö6983 (Protein Kinase C inhibitor), CGP77675 (SFK inhibitor), Y27632 (Rho-associated Kinase inhibitor), BIRB796 (p38-MAPK inhibitor), LIF (20 ng/mL), Activin A (10 ng/mL) and Geltrex (0.2%). This method enables the generation of human naive stem cells without the use of broad HDAC inhibitors that often results in the appearance of additional off target cell types. Stabilizing the naive pluripotent state is also more prolonged with the latter approach as HDAC inhibition requires at least 5 passages for the stabilization of the pluripotent state (G. Guo et al., 2017). Another advantage of the HENSM condition is that it does not require the use of mouse embryonic fibroblast (MEF) feeder layers. This reduces the variability in application and difficulty in gene targeting applications (Bayerl et al., 2021). Despite the advancements in the field, there are still a number of issues regarding the acquisition of naive PSCs in the culture dish. One of the issues is that, compared to the actual preimplantation epiblast cells, there is still a greater level of DNA methylation present in the naive cells acquired in vitro. While certain culturing methods can achieve a more drastic reduction in the global DNA methylation, this often comes at the expense of karyotypic abnormalities (Bayerl et al., 2021). Additionally, compared to the primed PSC culture conditions, the cells are much less stable under the naive culture conditions (Pastor et al., 2016). Even though it has been shown that PXGL and HENSM conditions do not usually cause karyotypic abnormalities after prolonged passaging, the long-term culture with MEK inhibition eventually leads to loss of imprinting. Therefore, improved conditions that would support and maintain human naive pluripotent stem cells is necessary (Oldak et al., 2023).

1.3 Somatic cell reprogramming

In 1957, CH Waddington described the idea of an epigenetic landscape which depicted the concept of development as a ball rolling down a hill going into different valleys, likening the state of the ball to a state with high potential and valleys as the terminally differentiated state. According to this idea of development, Waddington proposed that the axis of development is unidirectional, meaning that once the cells reach a final differentiated state, they cannot go back uphill in the developmental trajectory (Waddington, 2014). While this hypothesis was believed to be correct initially, different clues suggesting that cell identity can be forced to go back to a less mature state have

been described in the years following Waddington's work. In 1958, John Gurdon performed an experiment in which he removed the nucleus of a fertilized frog egg and replaced it with the nucleus of a cell from the intestine of a tadpole. After this replacement, the cell with the replaced nucleus grew to become a new frog showing that mature cells have the necessary genetic material to give rise to all of the tissues and that development potential can be unlocked with the right stimuli from the environment (Gurdon et al., 1958).

In 2006, inspired by the work of John Gurdon, Shinya Yamanaka showed that, by introducing only four transcription factors: OCT4 (Octamer-binding transcription factor 4), SOX2 (SRY-box transcription factor 2), KLF4 (Krüppel-like factor 4) and c-MYC into somatic fibroblast cells, one can reset the somatic identity acquired during development completely and awaken an endogenous pluripotent state. In their work, they first overexpressed 24 factors individually and in combination in mouse embryonic fibroblasts. They observed that while no single factor can successfully reprogram fibroblasts, a combination of all 24 factors could reprogram MEFs. Then, they determined which factors are crucial for this process to occur successfully. After screening four the most necessary candidates, they identified the four factors, which are now called Yamanaka factors (Takahashi & Yamanaka, 2006).

Reprogramming takes place in three phases. These steps include early (initiation) intermediate, and late (maturation and stabilization) phases. In the early phase after the OSKM expression, cells will increase proliferation, downregulate the expression of somatic genes, initiate the mesenchymal-to-epithelial transition (MET). At this point, the cells that are reprogrammable will enter the intermediate phase. In this phase, there are several, as yet unidentified barriers that limit or delay the acquisition of the pluripotent state. Additionally, cells will activate pluripotency markers in a stochastic manner along with a metabolic switch towards glycolysis. In the late phase, the stabilization of the pluripotency occurs. The transgenes that are used for the induction are silenced. The endogenous pluripotency genes become active. In addition to the complete reset of the epigenome, the cytoskeleton is rewired in line with the acquired iPSC fate. The resulting cells are named induced pluripotent stem cells (iPSCs) and possess the same developmental potential as embryonic stem cells (Buganim et al., 2013).

1.4 Chromatin Based Barriers of Reprogramming

After the discovery of reprogramming, several reports suggested that low efficiency (on the order of 0.01 to 0.1 %) can be overcome by utilizing small molecules that target the certain chromatin-based barriers towards successful iPSC derivation. One of those barriers is DNA methylation. DNA methylation is mainly a hallmark of gene repression. Guo et al. have shown that knocking down Dnmt3a and Dnmt3b improves the efficiency of reprogramming (X. Guo et al., 2013). In another study, targeting another DNA methyltransferase, DNMT1, showed that knockdown or small molecule inhibition of DNMT1 leads to enhanced efficiency of reprogramming (Mikkelsen et al., 2008). The barrier effect of DNA methylation in reprogramming has also been detected in studies dissecting the Ten-eleven Translocation proteins which carry crucial roles in DNA demethylation. Hu et al. showed that, in the absence of TET1-3, the cells in the early stages of reprogramming fail to undergo MET (Hu et al., 2014). In fact, the necessity of the demethylating activity of TET family has also been highlighted in a study published by Gao et al. which showed that TET1 promotes OCT4 methylation which resulted in successful reprogramming with only SKM factor without the need for exogenous OCT4 (Gao et al., 2013).

Different histone modifications have also been implicated as barriers of reprogramming. H3K9 methylation has been shown to be a barrier in reprogramming in different reports. It has been shown that lowering this mark has a positive effect on the reprogramming efficiency either via the knockdown or inhibition of its “writers” such as Ehmt2. In fact, the reduction of this mark relieves the chromatin which makes it easier for the OSKM factors to bind to several pluripotency associated genes (Sridharan et al., 2013). Additionally, H3K4 methylation is another histone modification that has been implicated during reprogramming. It has been suggested that H3K4me2, which is associated with gene activation, is deposited dramatically during the initial stages of reprogramming (Koche et al., 2011). In fact, when the removal of the H3K4me2 mark is inhibited, the somatic identity related genes’ expression levels are reduced and pluripotency related gene expression levels are upregulated, resulting in an increased reprogramming efficiency (Cacchiarelli et al., 2015). In addition to the mentioned histone modifications, H3K79 methylation was discovered to be a barrier in reprogramming showing that the inherently low reprogramming efficiency can be improved with the help

of small molecule inhibitors for the first time. Onder et al. showed that genetic and pharmacological inhibition of DOT1L, which is the writer of the H3K79me3, increases the efficiency of reprogramming and enables reprogramming without KLF4 and cMYC (Onder et al., 2012). After the initial discovery, the DOT1L inhibition has been reported to facilitate reprogramming in a wide range TF-mediated reprogramming approaches (Arabacı et al., 2021). Moreover, it has also been shown that DOT1L inhibition is necessary for the chemical reprogramming of both mouse and human fibroblasts without the use of any exogenous factors (Guan et al., 2022; Hou et al., 2013).

One of the key ways chromatin modifiers represents barriers in reprogramming is via maintaining the expression of genes associated with somatic cell identity. It has been shown that inhibition or knockdown of several chromatin modifiers such as FACT (facilitates chromatin transcription) (Kolundzic et al., 2018), DOT1L (Onder et al., 2012), SUMO (Cossec et al., 2018), BRD9 (Sevinç et al., 2022) and CBP/EP300bromodomain (Ebrahimi et al., 2019) leads to enhanced efficiency in reprogramming via the downregulation of the somatic cell associated gene transcription downregulation.

1.5 Screening approaches for identifying barriers of somatic cell reprogramming

There have been a number of studies investigating the barriers of reprogramming via the utilization of large screens. In 2012, Onder et al., via the utilization of short hair-pin RNAs targeting chromatin-modifying proteins, showed that while the knockdown of polycomb repressive complex 1 and 2 components such as EZH2 reduced the reprogramming efficiency. In contrast, the knocking down SUV39H1, YY1 and DOT1L enhanced the reprogramming of human fibroblasts. In fact, in the same paper, Onder et al. utilized a small molecule inhibitor of DOT1L which led to a similar increase in reprogramming providing a method of increasing the inherently low efficiency of reprogramming without genetic interference (Onder et al., 2012). In another study, Yang et al. reported the use of a genome-wide shRNA screen. In this screen, they identified Tfdp1, Gtf2e1, Nfe2, Foxn3, Erf, Cdkn2aip, Msx3, Ssbp3, Dbx1, Hoxd4, Lzts1, Arx, Hoxd12, Gtf2i, Ankrd22 and Hoxc10 to be barriers of reprogramming. In the same screen, they also identified several important factors for generating mature iPSC colonies such as Utf1 and Tdgf1 (Yang et al., 2014). Qin et al. applied a similar shRNA screen approach, with which they identified a disintegrin and metalloproteinase (ADAM) family proteins

are barriers of reprogramming. They also reported that the disintegrin domain is crucial and sufficient for the barrier function. In addition to the ADAM family proteins, they discovered that UBE2E, UBE2D, RNF40, DRAM1, SLC17A5, ATF7IP, MED19, TTF2 and TMF1 are barriers to human fibroblast reprogramming(Qin et al., 2014). Using a different shRNA screen targeting 670 epigenetic modifiers, Miles et al. observed that TRIM28 is a negative regulator of reprogramming by keeping the H3K9me3 repressed and preventing the endogenous retroviruses from getting activated (Miles et al., 2017). In a more recent paper, Ulrich Elling's group, suggested the use of a novel method for screening for reprogramming barriers. In their screen, they labeled the mouse embryonic fibroblasts using unique molecular identifiers (UMIs) and searched for genes limiting the efficiency of reprogramming. In this screen, they showed that two genes Men1 and Pias1 which encodes an E3 SUMO-protein ligase limits the efficiency of reprogramming dramatically (Michlits et al., 2017). In a mouse reprogramming screen, SUMO2 was identified to be a hit that prevents the reprogramming of mouse cells (Borkent et al., 2016). Toh et al. showed that SMAD3 (TGF-β pathway), ZMYM2 (epigenetic modifier), SFRS11 (splicing factor), SAE1 (Sumo-activating enzyme) and ESET (H3K9 methyltransferase) are barriers of human somatic cell reprogramming which they discovered via the utilization of a genome wide siRNA screen (Toh et al., 2016). In another paper, Pfaff et al. identified that miRNA-212/132 imposes a barrier in reprogramming in mice (Pfaff et al., 2017). Miles et al., utilizing an shRNA screen with a particular focus on epigenetic modifiers observed that TRIM28 and SETDB1 are barriers in reprogramming by establishing H3K9me3 which maintain the somatic cell identity (Miles et al., 2017).

While the genetic approaches for determining the barriers of somatic cell reprogramming have proven greatly useful, several groups attempted to perform small molecule inhibitor screens for identifying methods to enhance the efficiency of reprogramming without the genetic modifications. Huangfu et al. showed that 5'-azactydine (DNA methyltransferase inhibitor) and broad HDAC inhibitors suberoylanilide hydroxamic acid (SAHA), trichostatin A (TSA), and valproic acid (VPA) increase the efficiency of reprogramming (Huangfu et al., 2008). Li et al. identified in their kinase inhibitor screen that small molecule inhibitors that target p38, inositol 3-kinase and Aurora A kinase increase the reprogramming efficiency (Li & Rana, 2012). In 2019, Ebrahimi et al. performed a chemical screen containing inhibitors of chromatin

factors. With the help of this screen, they identified acetyl-lysine competitive inhibitors targeting the bromodomains of coactivators CREB (cyclic-AMP response element binding protein) binding protein (CBP) and E1A binding protein of 300 kDA (EP300). One of the two inhibitors that they discovered, CBP30, was recently utilized in the chemical reprogramming of human cells to pluripotency (Ebrahimi et al., 2019).

In addition to the screens described in the literature, our group had performed a CRISPR-Cas9 based screen for human somatic cell reprogramming. To determine the reprogramming barriers whose absence or inhibition can be combined with DOT1L inhibition, a pooled screen was performed, with a particular focus on chromatin modifiers. During the screen, 247 histone modifier-coding genes' functional domains were targeted, for each receiving 5 or 10 gRNAs. As control, 80 non-targeting gRNAs were also included. Human fibroblasts were transduced with lentiviruses containing gRNA expressing plasmids in addition to the already expressed Cas9. After 14 days since the beginning of reprogramming with OSKM factors, TRA-1-60 positive cells were sorted. Genomic DNA was extracted and gRNAs were amplified to add sequencing adapters at the ends of PCR products. After deep sequencing of fragments, gRNAs were aligned to the genome to get raw count data. MaGECK algorithm was used to detect enriched gRNAs and target genes inTRA-1-60 positive cell population compared to day 0 of reprogramming. In addition to some of the well-known or studied chromatin barriers, *MLL1* gene was identified to be a chromatin barrier of somatic cell reprogramming (Aztekin, 2016)

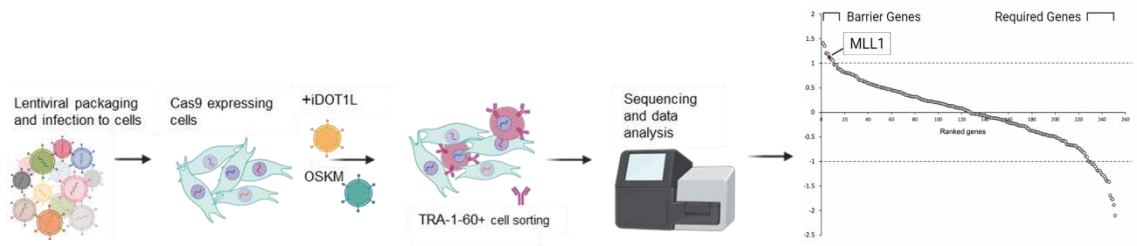

Figure 1.1. Schematics of screen. Y-axis represents the LogFC enrichment score for genes. X-axis represents the ranked genes in the library. MLL1 is highlighted among genes whose gRNAs are enriched in the TRA-1-60 sorted population.

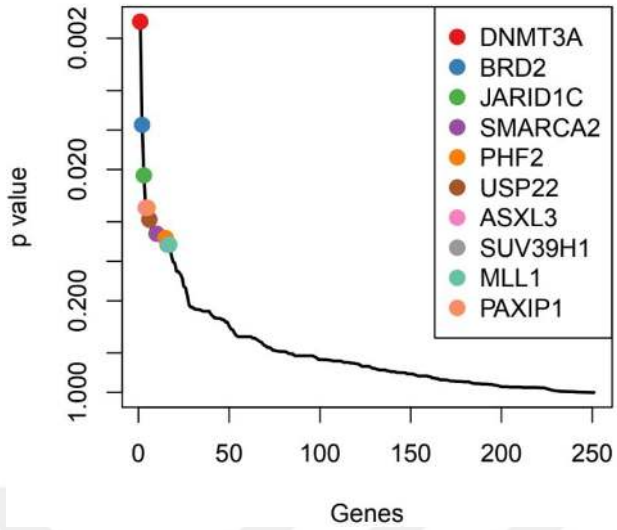

Figure 1.2. Screen results from D14 of reprogramming.

1.6 The proteins MENIN and MLL1

MLL1 (Mixed Lineage Leukemia 1, also known as *KMT2A*) is a gene that has been discovered as the homolog of trithorax gene found in Drosophila. MLL1 is responsible for the positive regulation of the HOX gene expression and H3K4 methylation (Krivtsov & Armstrong, 2007). It has also been shown that MLL1 carries critical roles in embryonic development, one of which is to retain an "epigenetic memory" of the cell identity during development (Blobel et al., 2009). In fact, complete ablation of MLL1 leads to embryonic lethality in mice at E11.5-14.5 (Milne, 2017; Yagi et al., 1998). MLL1 is also a proto-oncogene. In the case of its translocation, it forms leukemogenic fusion proteins that hyperactivate normal MLL1 target genes and prevent hematopoietic cell differentiation (Krivtsov & Armstrong, 2007). Due to its role in the development of acute leukemia, several compounds for inhibiting the MLL activity have been developed. Recently, it has been shown that a compound called MM-401, which was initially developed to inhibit the interaction of MLL1 with WDR5, has been shown to facilitate the reversion of the primed mouse ESCs back to the naive pluripotent state. Zhang et al. reported that inhibiting the MLL-WDR5 interaction and knocking out MLL1 lead to the downregulation of differentiation commitment genes which in return leads to the derepression of the naive pluripotency circuitry (Zhang et al., 2016).

One of the key interaction partners of MLL1 is a protein called MENIN. MENIN is a protein encoded by the *MEN1* (Multiple endocrine neoplasia 1) gene. This gene has been shown to be mutated in patients with multiple endocrine neoplasia type 1 (MEN1) syndrome. This syndrome distinguishes itself via the tumor formation in endocrine organs such as the pituitary gland, the parathyroid gland and the pancreatic islets. The patients who inherit this disease usually have one germline mutation in the *MEN1* gene, and undergo loss of heterozygosity in the endocrine tumors. Therefore, MENIN acts as a tumor suppressor in endocrine tissues. Tumor-associated *MEN1* mutations are not restricted to specific residues. The tumor suppressor role of MEN1 has also been shown in the context of different tissues such as pancreatic endocrine and sporadic parathyroid tumors. However, Menin have opposing roles in cancer development across different tissues (Matkar et al., 2013). Menin has crucial roles acting as the promoter of MLL and MLL-fusion protein increases in HOX gene targets and H3K4 trimethylation. In fact, inhibitors of Menin have shown to be successful in the subset of preclinical leukemia models. This tumor promoter effect is also present in the context of the prostate cancer. In prostate cancer, the MLL1-MENIN complex co-activates the androgen receptor (Katona et al., 2019).

MEN1 plays important roles in development as well. It has been reported that complete *Men1* ablation in mice leads to embryonic lethality due to multiple organ deficiencies at E11.5-E13.5 (Matkar et al., 2013). Bertolino et al. showed that *Men1* null mutant embryos are smaller in size in addition to having hemorrhages and edemas at a frequent rate. Moreover, a large number of the embryos have defects in the closure of their neural tubes. These defects are accompanied by the disorganization of the epithelial and hematopoietic compartments in the liver which is associated with greater levels of apoptosis. Interestingly, they reported that *Men1* null ES cells have shown deficiencies in generating embryoid bodies despite having comparable proliferation rates with the control cells in culture. These findings suggest that *Men1* gene plays crucial roles in differentiation across different tissues during development (Bertolino et al., 2003).

MENIN protein contains 610 amino acid residues. While it is conserved from Drosophila to humans, it is not present in yeast or *C. elegans*. This suggests that the *MEN1* gene, evolutionarily speaking, is relatively a new gene. As mentioned earlier, it has crucial roles during the embryonic development with roles in different tissues, even opposing roles across different tissues. A good example of this dual activity is that while Menin

acts as a tumor suppressor in the endocrine tissues, it is required for leukemogenesis. This duality stems from the fact that Menin has the ability to act as a scaffold protein. Scaffold proteins are defined as proteins that can bring together two or more proteins into a stable configuration and enhance signaling efficiency and fidelity. Due to this characteristic, Menin can bind different proteins such as MLL1 and JUND but the resultant effect of this binding is dramatically different. While MLL1 binding leads to active transcription, JUND binding leads to suppression of JUND-induced transcription (Matkar et al., 2013). The active transcription activity of MLL1-MENIN complex is dependent on the presence of another protein PSIP1 (also known as LEDGF). Yokoyama et al. showed that MENIN links MLL1 with PSIP1 which is a requirement for MLL1-dependent transcription (Yokoyama & Cleary, 2008). Additionally, the effect of *Men1* ablation in reprogramming has been demonstrated in mouse embryonic fibroblast cells previously. In these two papers, Men1 has come up as a screen hit as a reprogramming barrier. In one of those reports, it was suggested that the Menin is involved in shielding the cell identity (Kaemena et al., 2023; Michlits et al., 2017). While neither of these papers suggested a mechanism by which Menin is a reprogramming barrier, they both reported that its depletion increases reprogramming efficiency significantly. More recently, MENIN-MLL inhibitor, VTP50469 has been utilized in the chemical reprogramming of human dermal fibroblasts and adipose derived stem cells (Guan et al., 2022). These studies suggest that protein Menin plays a crucial role as a barrier in somatic cell reprogramming.

A recent paper showed Menin protein is a “reader” of the H3K79me2 mark. In this paper, Lin et al. reported that Menin recognizes the H3K79me2 mark in addition to the pocket domain that recognizes Mll1 which has been established previously. They showed how Menin recognizes this mark to bind to the nucleosome and identified a mutant that can’t recognize the H3K79me2 mark (Lin et al., 2023).

Menin-Mll1 interaction has been studied to advance the therapeutic applications for leukemia. The leukemogenic fusion proteins work by binding to chromatin and induce leukemic transformation via the deregulation of its target genes. These target genes include *HOXA* genes and their co-factors such as *MEIS1* which has been implicated in leukemia development, proliferation and self-renewal (Krivtsov & Armstrong, 2007). Yokoyama et al. showed that Menin is critical for the maintenance of MLL fusion protein driven gene expression. The critical role of Menin is due to its binding to a five amino acid sequence near the N terminus of MLL1. In the absence of this binding, expression

of *HOXA* genes are impaired, which leads to growth arrest and differentiation (Yokoyama et al., 2005). For this purpose, several small molecule compounds that inhibit the MENIN/MLL interaction have been developed. In 2019, Krivtsov et al. showed that, with a new small molecule inhibitor named VTP50469, Menin-Mll1 complex can be inhibited in potent selective and potent manner. Interestingly, in their paper, they showed that inhibiting the Menin-Mll1 complex leads to a decrease in protein levels of Menin and Dot1L. Additionally, the expression levels of the key fusion protein target genes such as *MEIS1* and *PBX3* are downregulated.

In this thesis, I first identified that Mll1 acts a barrier via its interaction with Menin. I showed that a potent and specific Menin-Mll1 inhibitor, VTP50469, enhances the efficiency of reprogramming. This significant enhancement can be utilized in different settings that require the generation of personalized iPSCs lines for studying disease and development or in the clinic. Additionally, I showed that deletion of the *MEN1* gene leads to greater levels of increase in reprogramming compared to the inhibitor treatment. This suggests that Menin imposes barrier functions that are not related to its interaction with Mll1. We also hypothesized that MLL1-MENIN complex might have repressive functions on pluripotency. To test this paradigm, I performed naïve conversion of different PSC lines in the presence of MLL1-MENIN inhibitor. We observed that cells increase expression of marker genes of the "naïve" state when they are treated with VTP50469. This shows MLL1-MENIN complex may also have repressive roles on pluripotency.

Chapter 2:
MATERIALS AND METHODS

2.1 Cloning and transformation

Enzymatic digestion of LentiCRISPR-v2 (Addgene plasmid, #52961) plasmid was performed with BsmB1 (NEB). Following the gel electrophoresis, the 12,988 bp size band was purified with MN PCR Clean Up and Gel Extraction Kit. The extracted linear vector was treated with Antarctic Phosphatase. The specific top and bottom guide RNA sequences were taken from the GeCKO Library (Table 2.1). Each gRNA oligo (100 µM) was annealed with T Polynucleotide Kinase) and T4 DNA Ligase Buffer (NEB). A total of 10 µl reaction was set at 37°C for 30min, 95°C for 4 min and then the temperature was ramped down to 25°C at a rate of 5°C/min in a thermal cycler. Diluted (1:200) oligos were used as inserts for ligation reaction mixes which include 50 ng digested LentiCRISPR-v2 plasmid. The reactions were incubated at RT for 2 hours. For each reaction, ligation reaction was mixed by vortexing following which 5µl of the reaction was transferred into 50 µl competent bacteria aliquot that was thawed on ice. The mixture was incubated for at least 30 minutes on ice then heat shock was performed at 42°C for 30 seconds in a water bath. Eppendorf was replaced on ice to normalize temperature for 5 minutes before adding 150 µl SOC medium. Transformation mixture was cultured at 37°C and 225 rpm in orbital bacterial shaker. 60 minutes later, 100µl growth culture was spread on Ampicillin resistant LB agar plate. Clones were confirmed by U6 promoter targeted Sanger sequencing. gRNAs targeting *MLL1* were previously cloned (Çimen, 2018).

Table 2.1. The table of gRNAs used in cloning.

MEN1_1_Top	CACCGCATGCGCTGTGACCGCAAGA
MEN1_1_Bottom	AAACTCTTGCGGTCACAGCGCATGC
MEN1_2_Top	CACCGCCAGGCATGATCCTCAGACA
MEN1_2_Bottom	AAACTGTCTGAGGATCATGCCTGGC
MLL1_1_Top	CACCGCCGGTAGCGTAGCAAATGGC

MLL1_1_Bottom	AAACGCCATTTGCTACGCTACCGGC
MLL1_2_Top	CACCGCAGCAGCCTTTAGATCTAGA
MLL1_2_Bottom	AAACTCTAGATCTAAAGGCTGCTGC
MLL1_3_Top	CACCGTTGTAGGATGAGCAATTCTT
MLL1_3_Bottom	AAACAAGAATTGCTCATCCTACAAC
MLL1_4_Top	CACCGCCACCCTGAGTGCCTTACCA
MLL1_4_Bottom	AAACTGGTAAGGCACTCAGGGTGGC

To create MEN1 g2 resistant cDNA, point silent mutation to destroy the NGG site was performed on pBABE Hygro WT MEN1 (Addgene plasmid, #11024). The NGG site was destroyed via the Q5 Site-Directed Mutagenesis Kit. The acquired plasmid was used for creating additional point mutations A242V, P12L, H139D, E255K, T344R with Q5 Site-Directed Mutagenesis Kit. The mutations were confirmed by Sanger sequencing.

Table 2.2. The table of primers used for Q5 site directed mutagenesis.

MEN1_11024_PAM_Mutation_F	TGTCCACCTCGCACTGTCTGAGG
MEN1_11024_PAM_Mutation_R	TCCCGGAGACCCAGGGCC
MEN1_11024_P12L_F	ACGCTGTTCCTGCTGCGCTCC
MEN1_11024_P12L_R	CTTCTGGGCGGCCTTCAG
MEN1_11024_T344R_F	TGGGCGGACAGGGCCACTGTCATCCAGG
MEN1_11024_T344R_R	GGCCTGCAGGGCTTCCCGCACATTGC
MEN1_11024_A242V_F	ATGGTGTGTGTCATCAACCCT
MEN1_11024_A242V_R	GAACGCCACCTCCATCTT
MEN1_11024_H139D_F	GGATCGGGCCGACATCCAGTC
MEN1_11024_H139D_R	TTGAAGTAGGAGCGGCTG
MEN1_11024_E255K_F	CGACTCGCTGAAGCTTCTGCA
MEN1_11024_E255K_R	GTGTGCAGGTCAATGGAAG

2.2 Plasmid DNA Isolation

Single bacteria colonies that were grown on LB agar plates were picked into 200 mL LB Broth with respective antibiotics. The suspension cultures were grown at 37°C and 225 rpm in a bacterial orbital shaker. After overnight incubation, the bacterial cultures were transferred to the conical tubes and centrifuged at 4°C and 3750 rpm for 30 minutes. The supernatants were removed. The plasmid isolation from the pellets was performed using the Macherey-Nagel (MN) Midi Prep Kit. If the plasmid DNA was isolated from commercial stab bacteria culture (Addgene), the culture was started by streaking the bacteria for generating single colonies. The plasmid isolation was performed as mentioned.

2.3 Supernatant and concentrated virus production

$2x10^6$ HEK 293T cells were seeded in D10 (10% FBS, 1% Pen-Strep in DMEM High Glucose) medium onto 10 cm cell culture plates. The next day, the cells were transfected with the mix of the viral packaging plasmids (250 ng of the envelope protein encoding plasmid (VSV-G), 2250 ng Gag-Pol (pUMVC for retroviruses and psPAX2 for lentiviruses) and 2500 ng viral plasmid DNA using FuGENE® 6 Transfection Reagent (Promega). The plasmids and transfection reagent were mixed serum free DMEM in different tubes with a total volume of 200 µL. After waiting for 5 minutes for the transfection reagent to get activated, the plasmid mix and the transfection reagent mix were combined and incubated at room temperature for 30 minutes. At the end of the incubation, the mix is added into the HEK 293T cell culture medium. The supernatants were collected into conical tubes at 48 and 72h. These tubes were then centrifuged and filtered with 0.45 syringe filters to exclude any HEK 293T cell debris. After these steps, the supernatants were either concentrated or aliquoted and stored as they were. For concentration, the filtered supernatant is combined with 50% PEG8000 at 1:4 ratio and mixed. After 48 hours, the conical tubes were centrifuged at 4°C. The pellet was resuspended with PBS at a concentration of 100x.

2.4 Fibroblast viral infection

Fibroblast cells were seeded as 1x10^5 cells per well of a 6 well plate. The next day, the cells were infected with 1 mL virus supplemented with 200 µL fresh D10 medium and proteamine sulfate (8 µg/mL). The following day, the infection was repeated. After the infections, the cells were split at a 1:3 ration following which blasticidin (7 µg/mL), puromycin (1 µg/mL) or hygromycin (50 µg/mL) selection was performed. Fibroblast cells were counted and seeded at specific ratio (1x10 5 cells/ well into 6 well plates). Cells were infected with 1 ml viruses, 200µl fresh medium and protamine sulfate (8 µg/ml) after 24 hours from seeding. Next day, the infection was repeated (optional). After infections, cells were split at 1:3 following which puromycin selection was performed (1 µg/ml).

2.5 Preparation of inactivated mouse embryonic fibroblasts for stem cell culture

At E13.5, pregnant C57BL/6 mice were sacrificed by cervical dislocation. The embryos were separated from the surrounding membranes, placenta, brain and other red organs. Blood was removed by washing with PBS. After separation, the embryos were minced finely with a razor blade until they were pippettable. Each embryo was resuspended in 2 mL of 0.05% trypsin-EDTA and incubated at 37°C for 15 minutes. Then, trypsin-EDTA was inactivated by adding 4 mL D10 (10% FBS, 1% Pen-Strep in DMEM High Glucose) before removing any remaining large pieces. After centrifugation at 1500 rpm for 5 minutes, the pellet was resuspended in 5 mL D10 media per embryo. Two embryos were plated at Passage 0 on a gelatin coated 10 cm plate (0.01% gelatin). After MEFs reach confluency, customized MEF (cMEF) medium (20% FBS, 1% NEAA, 1 mM Sodium Pyruvate, 1% Pen-Strep, 0.1 mM 2-mercaptoethanol in DMEM High Glucose) was used to grow and expand the cells. For passaging, cells were washed with PBS once. Then, 2 mL 0.05% trypsin-EDTA was added. After 5 minutes of incubation at 37°C, 4 mL cMEF medium was added for trypsin inactivation. The cells were split at ratios of 1:4-1:5 until passage 3. After the cells reach 80-90% confluency at passage 3, inactivation via irradiation was performed. Irradiation was performed using Strahl CIX2 irradiator. For inactivation, cells received 30–40 Gy using the 3.00 Al filter for 30 minutes. Following irradiation, plates are placed back into the incubator for at least an hour for recovery before freezing. At the end of the recovery incubation, cells are trypsinized and

frozen using the freezing medium (90% FBS and 10% DMSO). Cryovials are transferred to the nitrogen tank after 24 h in the -80°C.

2.6 Episomal nucleofection and reprogramming

For reprogramming with episomal plasmids, pCXLE-hOCT3/4-shp53-F (Addgene plasmid, #27077), pCXLE-hUL (Addgene plasmid, #27080), pCXLE-hSK (Addgene plasmid, #27078). Each plasmid (5 µg total) was electroporated into $1x10^6$ human adult fibroblasts using the Neon electroporation kit. Then, fibroblasts were seeded as $5x10^4$ into each well of a 12 well plate. The culture media was changed every other day with D10 until Day 6 after nucleofection. On Day 6, the cells were split at 1:8 ratio onto inactivated MEFs. The next day, the media was changed from D10 to human embryonic stem cell media. Media was changed every day until iPSC colonies became large enough.

2.7 Cell surface marker TRA-1-60 PE staining and flow cytometry

This assay was performed as described earlier (Sevinç et al., 2022) using PE-conjugated anti-human TRA-1-60-R antibody (Biolegend, catalog no. 330610) at a dilution of 1:400.

2.8 TRA-1-60 HRP DAB staining, quantification and ImageJ Analysis

The number of human iPSC colonies were quantified via TRA-1-60 immunostaining. Paraformaldehyde-fixed cells were washed with PBS thrice and incubated with biotin-anti-TRA-1-60 (comp) at 1:250 dilution in the staining solution consisting of 3% FBS, 0.3% Triton-X-100 in PBS overnight at 4°C. The following day, cells were washed twice with PBS and incubated with streptavidin horseradish peroxidase (comp) at 1:500 dilution for 2 hours at room temperature. A master mix of DAB solution was prepared by adding and vortexing in DAB solution 0.1% 3,3'-diaminobenzidine, 0.05% nickel ammonium sulfate and 0.015% hydrogen peroxide. Brown color was present after 10 minutes of incubation with the DAB solution. Following the color development, the cells were washed with PBS twice. Heavy cream was added onto the plates to create the contrast between iPSC colonies and their surroundings. The plates with added heavy cream were then scanned in JPEG format with an at least 600 dpi resolution. The scanned images were analyzed with ImageJ (https://imagej.nih.gov/ij/).

2.9 Nuclear Protein Extraction

Since MENIN is largely a nuclear protein, nuclear protein extraction was performed. The cell pellets were first resuspended in the cytosolic lysis buffer (10 mM HEPES, 10 mM KCl, 0.1 mM EDTA, 0.4% NP-40, protease inhibitor in dH2O with pH 7.9). The resuspended pellets were shaken on ice for 15 minutes. Then, the samples were centrifuged at 3000 g for 3 minutes at 4°C. The supernatant is removed and the remaining pellet is resuspended with the cytosolic lysis buffer again. After resuspension, the samples were centrifuged again at 3000 g for 3 minutes at 4°C. The supernatant is removed for the last time for clearing the sample off of cytosolic proteins. Then, the remaining pellet is resuspended with the nuclear lysis buffer (20 mM HEPES, 0.4 M NaCl, 1 mM EDTA, 10% Glycerol, protease inhibitors in dH2O with pH 7.9). Then the samples were sonicated with 10 seconds on, 30 seconds off program that is repeated four times. The sonicated samples were centrifuged at 15,000 g for 5 minutes. The supernatant is collected and stored in -80°C until use. The protein concentrations for the samples were determined using the Pierce BCA Protein Assay Kit (Thermo Fisher Scientific, cat. #23225). 50 µg of each lysate was then boiled at 95°C for 15 minutes with 4X Laemmli buffer (Bio-Rad) supplemented with β-mercaptoethanol (Bio-Rad).

2.10 Western Blotting

The boiled samples (50 µg/well) and the protein ladder (Bio-Rad, cat. # 161-0374) were loaded onto pre-cast SDS-PAGE gels (Bio-Rad, cat. # 456-1084). Using the Bio-Rad trans-blot turbo transfer system at high molecular weight transfer settings, proteins were transferred onto a PVDF membrane (Bio-Rad, cat. # 1620177). Before the antibody incubation, the samples were blocked with 5% blotting grade blocker (Bio-Rad, cat. #1706404) solution for 1 hour. Then the membranes were incubated with anti-MENIN (Abcam, cat #31902) and anti-H3 Total (Cell Signaling, cat #4499) antibodies diluted 1:1000 overnight at 4°C. The following day, the membranes were washed with TBS-T for 15 minutes thrice. The washed membranes were then incubated with secondary antibodies (Abcam, cat. #ab97051) at 1:10000 dilution for 1 hour. Next, the membranes were washed with TBS-T for 15 minutes thrice and incubated briefly with ECL Western blotting substrate. The imaging of the membranes was performed with the Odyssey Imaging System (LICOR Biosciences).

2.11 Immunofluorescent staining and imaging

To perform immunofluorescent staining, cells were fixed with freshly prepared 4% paraformaldehyde (in PBS, with an adjusted pH of 7.4). After fixation, cells were washed with ice cold PBS thrice for 5 minutes each time. Then permeabilization was performed with PBS containing Triton X-100 (0.1%) for 10 minutes. At the end of the permeabilization step, cells are washed with PBS thrice. Following that, the samples were blocked with the blocking buffer containing 1% bovine serum albumin (BSA), 22.52 mg/ml glycine, 0.1% Tween-20 in PBS for 30 minutes at room temperature. Then, overnight incubation with the primary antibodies at the recommended dilutions was performed using the primary antibody staining buffer containing 1% BSA, 0.1% Tween 20 in PBS. Anti-KLF17 (Atlas, catalog number HPA024629), Anti-OCT4 (Abcam, catalog number ab19857), Anti NLRP2 (RND, catalog number MAB4684-SP) and LAMA4 (St. John's Laboratory, catalog number STJ93891) were used with concentrations of 1:250, 1:1000, 1:500, and 1:250 respectively. The next day, cells were washed with PBS thrice and incubated with secondary antibodies in the secondary antibody staining buffer (1% BSA in PBS) at room temperature for 1 hour. Then, the secondary antibody solution was removed and cells were washed thrice with PBS for 5 minutes each. To visualize the nucleus, DAPI staining (1 µg/ml in PBS) was performed for 5 minutes. The samples are washed for the last time for 5 minutes. Imaging was performed with Cytation 5 (BioTek).

2.12 Human primed reprogramming

Fibroblast cells were detached using 0.05% trypsin-EDTA solution. 50k cells were seeded into each well of a 12 well plate. The next day, the cells were infected with OSKM viruses with a total volume of 700 µL. The media change was performed with D10 every other day. On day 6 after OSKM infection, cells were splitted at a ratio of 1:8 and 1:16 onto vitronectin-coated plates (1:100). The next day after splitting, the culture media was switched to in-house made E7 media (L-ascorbic acid 2-phosphate magnesium salt (64 µg/ml), sodium bicarbonate (543 ng/liter), FGF2 (0.1 µg/mL), sodium selenite (0.014 µg/mL), holo transferrin (10.7 mg/liter), insulin (0.0194 mg/mL) and 1% Pen-Strep in DMEM/F12 base media). The media was changed every day until distinct colonies were formed. The plates were fixed with 4% paraformaldehyde for further analysis.

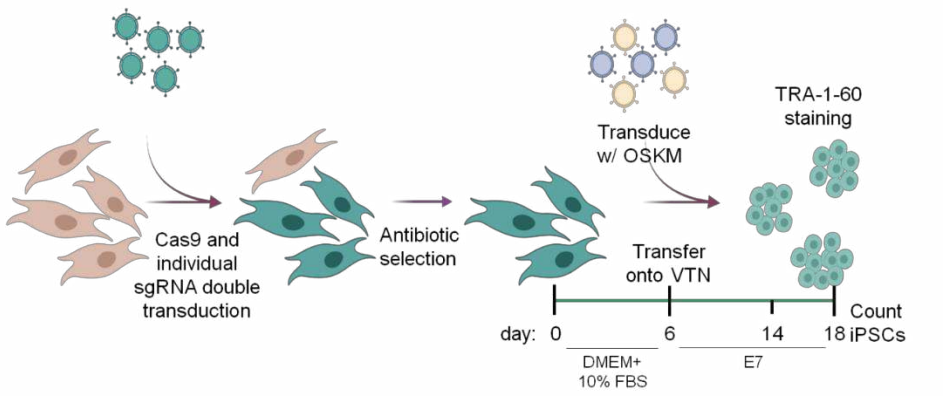

Figure 2.1. Schematics of human primed reprogramming

2.13 Human naive reprogramming

Fibroblast cells were detached using 0.05% trypsin-EDTA solution. 50k cells were seeded into each well of a 12 well plate. The next day, the cells were infected with OSKM viruses with a total volume of 700 µL. The media change was performed with D10 every other day. On day 6 after OSKM infection, cells were splitted at a ratio of 1:8 onto irradiated MEFs. The next day after splitting, the culture media was switched to HENSM-ACT (1% Pen-Strep (Biowest), 1% GlutaMAX (Gibco), 1% NEAA, 1 mM sodium pyruvate, 1% N2 supplement, 2% B27 supplement, 50 µg/mL L-ascorbic acid 2-phosphate magnesium salt, 0.2% Geltrex, 20 ng/mL hLIF, 2 µM XAV939, 2 µM Gö6983, 1.2 µM PD0325901, 1.2 µM CGP77675, 1.2 µM Y27632, 0.8 µM BIRB796, 10 ng/mL Activin A in a base media consisting of DMEM/F12 and Neurobasal combined at a ratio of 1:1) media. The media was changed every day until dome-shaped colonies became apparent. The plates were fixed with 4% paraformaldehyde for further analysis.

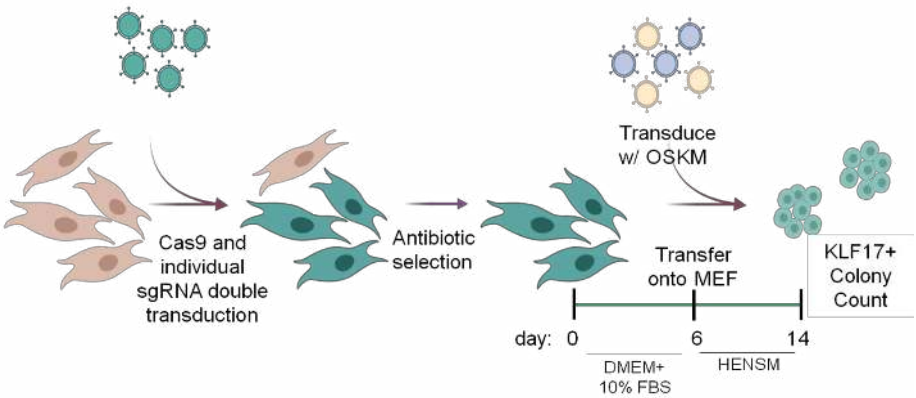

Figure 2.2. Schematics of human naive reprogramming

2.14 Primed to naive conversion

Naive conversion experiments were performed with the HENSM-ACT conditions using H9, WIBR3 OCT4 GFP, WIBR3 Delta PE OCT4 GFP and NO #2 PSC lines. After the primed PSCs were seeded onto 1% Geltrex coated plates in E8 medium, the media was switched to the HENSM-ACT which consists of 1% Pen-Strep (Biowest), 1% GlutaMAX (Gibco), 1% NEAA, 1 mM sodium pyruvate, 1% N2 supplement, 2% B27 supplement, 50 µg/mL L-ascorbic acid 2-phosphate magnesium salt, 0.2% Geltrex, 20 ng/mL hLIF, 2 µM XAV939, 2 µM Gö6983, 1.2 µM PD0325901, 1.2 µM CGP77675, 1.2 µM Y27632, 0.8 µM BIRB796, 10 ng/mL Activin A in a base media consisting of DMEM/F12 and Neurobasal combined at a ratio of 1:1. Dome-shaped morphology is acquired fully at passage 2-3 after the media switch. Passaging of naive cells were done by first washing the cells with PBS. Then, the cells were incubated with TrypLE (0.8x) for 3 minutes at 37°C. After 3 minutes, TrypLE was removed. The plate was airdried for 2 minutes. The loosely attached colonies were resuspended in the HENSM-ACT media containing 10 µM freshly added Y-27632. The cells were split at a ratio of 1:3-1:4 every 3 days.

2.15 RT-qPCR

This assay was performed as described earlier (Sevinç et al., 2022). The qPCR was performed by using SYBR-Green Master PCR mix (Roche) and run on a LightCycler480 Instrument II(Roche) with 40 cycles of 30 s at 95 °C, 30 s at 60 °C and 30 s at72 °C. All quantifications were normalized to an endogenous GAPDH control. The relative quantification value for each target gene compared to the calibrator for that target is expressed as $2^{(Ct-Cc)}$ (Ct and Cc are the mean threshold cycle differences after normalizing to GAPDH).

Table 2.3. The table of primers used for RT-qPCR

DPPA3 Forward	CGCATGAAAGAAGACCAACAAACAA
DPPA3 Reverse	TTAGACACGCAGAAACTGCAGGGA
DNMT3L Forward	CAGTGCCTGCTCCTTATGGCT

DNMT3L Reverse	TGAACAAGGAAGACCTGGACG
KHDC1L Forward	ACGAGTGCTCTCAGCAAGGA
KHDC1L Reverse	GTACGTGTCATCAAGTCCGAAGA
KLF17 Forward	AGCAAGAGATGACGATTTTC
KLF17 Reverse	GTGGGACATTATTGGGATTC
TFCP2L1 Forward	TCCTTCTTTAGAGGAGAAGC
TFCP2L1 Reverse	ACCAACGTTGACTGTAATTC
DPPA5 Forward	TGCTGAAAGCCATTTTCG
DPPA5 Reverse	GAGCTTGTACAAATAGGAGC
ARGFX Forward	CCGGAGTCAACAGTAAAGGTTTG
ARGFX Reverse	GGTGGGCACATTCTTCTTGGA
GAPDH Forward	CTCCTGCACCACCAACTGCT
GAPDH Reverse	GGGCCATCCACAGTCTTCTG
OCT4 Forward	CCTCACTTCACTGCACTGTA
OCT4 Reverse	CAGGTTTTCTTTCCCTAGCT
NANOG Forward	TGATTTGTGGGCCTGAAGAAA
NANOG Reverse	TGGTGGTAGGAAGAGTAAAG

2.16 Gene expression analysis and RNA Sequencing

For RNA sequencing, NT1, MEN1 and WT fibroblasts were used. WT cells received either DMSO or VTP50469 (1 μM) for 6 days after the OSKM induction. All of the experiments were performed under OSKM and no OSKM conditions. The cells were collected at D6. The RNA isolation was performed using the Nucleospin RNA Isolation Kit (Macherey Nagel) according to the manufacturer's instructions. RNA-sequencing was performed as 20 million reads per sample.

2.17 Statistical analysis

GraphPad Prism-10 was used for statistical analysis (t-tests and one way Anova tests). The details about replicates of samples are mentioned in the figure legends.

2.18 Data Availability

RNA sequencing data was registered in the NCBI GEO database.

Chapter 3:
RESULTS

3.1 CRISPR-Cas9 based screen identifies MLL1 as a barrier to reprogramming.

To validate the CRISPR-Cas9-mediated knockout screen results, individual gRNAs targeting the *MLL1* gene were cloned into the LentiCRISPR-v2 backbone. Human fibroblasts were infected with gRNAs and Cas9 expressing plasmids. After selection and 7 days in culture, cells were re-plated and reprogrammed to iPSCs with OSKM viruses. At the end of reprogramming, the number of colonies were quantified by TRA-1-60 staining. We showed that knocking out MLL1 in fibroblasts leads to significantly enhanced reprogramming efficiency (Figure 3.1) These results validated the MLL1 as a chromatin related barrier for somatic cell reprogramming. In addition, I observed that treatment of MLL1-KO cells with a DOT1L inhibitor (EPZ4777) resulted in further increase in reprogramming efficiency, suggesting that MLL1 and DOT1L may function as independent barriers to reprogramming.

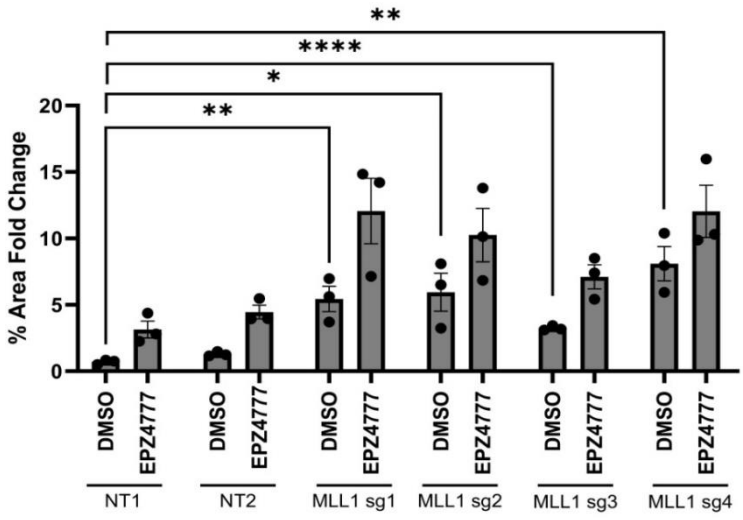

Figure 3.1. Fold change in percent area covered by TRA-1-60+ colonies at the end of reprogramming with fibroblasts expressing NT1, NT2 and 4 different gRNAs targeting *MLL1* gene. Error bars represent error of mean. n=3, independent experiments were conducted. Two-tailed t-test analysis was performed. * stands for $p \leq 0.05$, ** stands for $p \leq 0.01$, *** stands for $p \leq 0.001$, **** stands for $p \leq 0.0001$.

3.2 MLL1-MENIN interaction is critical for suppression of reprogramming

To determine if the MLL1 acts as a barrier to reprogramming via its interaction with Menin, we used a recently developed potent MLL1-MENIN inhibitor, VTP50469. Using this inhibitor, we first performed a time course experiment to determine if and when MLL1-MENIN complex prevents reprogramming to iPSCs. After treating cells with 0.33 μM VTP or DMSO as control for different durations at different time points, we have shown that this complex indeed represents a major barrier especially in the first 2 weeks of reprogramming (Figure 3.2). VTP50469 treatment throughout the first 14 days post-OSKM transduction resulted in a maximal 35.6-fold increase in reprogramming. Interestingly, treatment with VTP50469 during the late phases of reprogramming (7-14 or 14-18) had a much less effect.

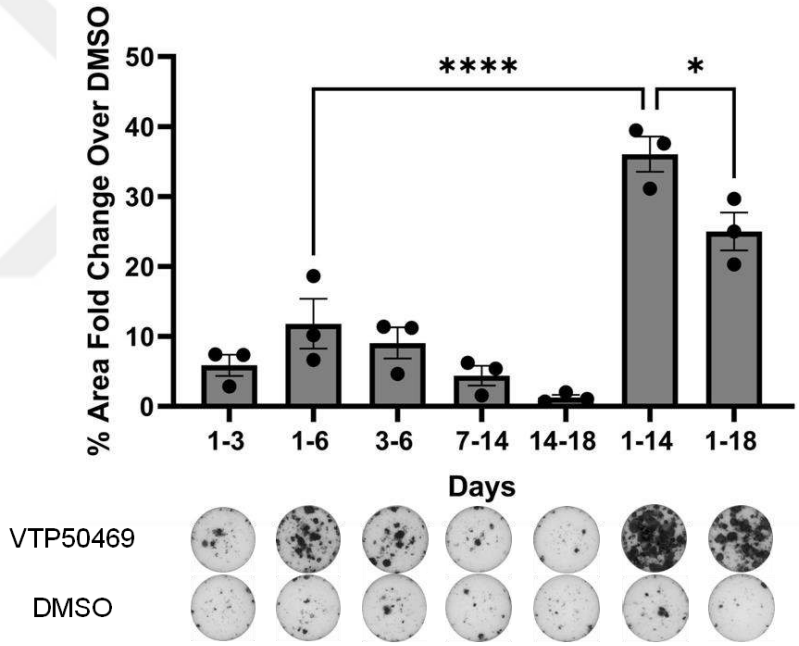

Figure 3.2. Fold change in percent area covered by TRA-1-60+ colonies after treatment with 0.33 μM VTP50469 for different durations and time points in reprogramming. Error bars represent error of mean. n=3, independent experiments were conducted. One way Anova analysis was performed. * stands for $p \leq 0.05$, ** stands for $p \leq 0.01$, *** stands for $p \leq 0.001$, **** stands for $p \leq 0.0001$.

Next, we aimed to determine the concentration to be used to maximize the efficiency enhancement. For this purpose, 0.1 μM, 0.33 μM, 1 μM, 3 μM and 10 μM of VTP

treatment was performed for the first 2 weeks of reprogramming. TRA-1-60 staining of these plates showed that 1 μM VTP is necessary for maximal effect of 28-fold increase in reprogramming compared to the DMSO (Figure 3.3).

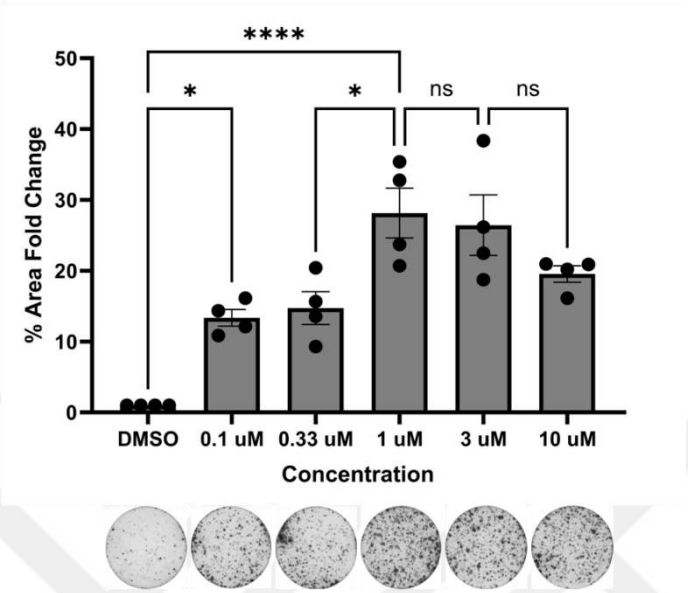

Figure 3.3. Fold change in percent area covered by TRA-1-60+ colonies after treatment with different concentrations of VTP50469. Error bars represent error of mean. n=4, independent experiments were conducted. Error bars represent error of mean. One way Anova analysis was performed. * stands for p≤0.05, ** stands for p≤0.01, *** stands for p≤0.001, **** stands for p≤0.0001.

To confirm the inhibitor results, a genetic approach was also utilized. Human fibroblasts were trasnduced with the lentiviral vectors expressing individual gRNAs targeting *MEN1* and Cas9. *MEN1* knockout in these fibroblast cell lines were confirmed via Western blot (Figure 3.4).

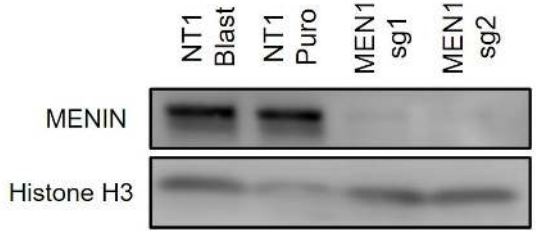

Figure 3.4. Western blot image showing MENIN protein level of MEN1 targeting gRNAs in fibroblasts. Histone H3 was used as a loading control.

MEN1 knockout cells were then plated and reprogrammed to iPSCs. The results showed that knocking out MEN1 leads to major enhancement in the reprogramming efficiency of human fibroblasts (Figure 3.5).

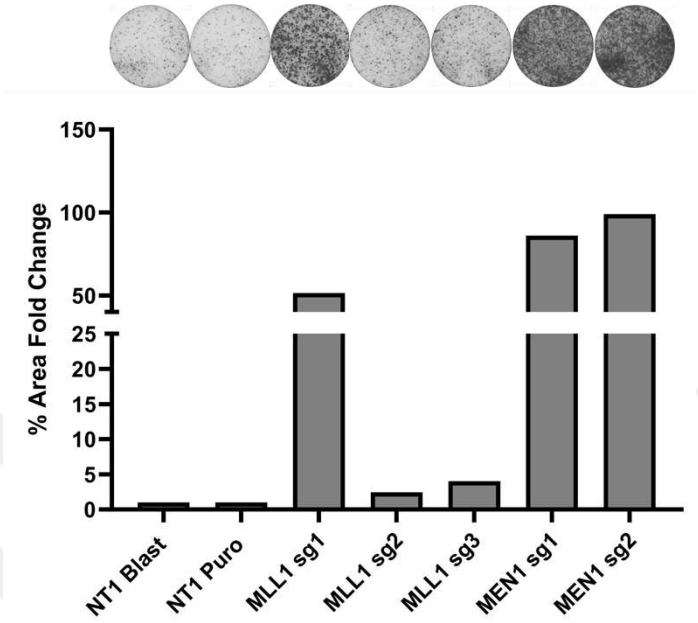

Figure 3.5. TRA-1-60 staining of the cells expressing *MEN1* and *MLL1*targeting gRNAs.

3.3 MENIN dependent transcriptional regulation during reprogramming

Due to significant enhancement of the reprogramming efficiency with MENIN inhibition and knockout, flow cytometry experiments were performed at day 6 after OSKM infection. For these experiments, TRA-1-60 antibody was used to detect the iPSCs cells formed early during reprogramming. These experiments showed that MENIN depletion both accelerates and enhances the emergence of Tra-1-60 positive cells close to 10-fold (0.49% for NT1 Blast vs. 4.85% for MEN1 KO) compared to control cells as early as day 6 of reprogramming (Figure 3.6).

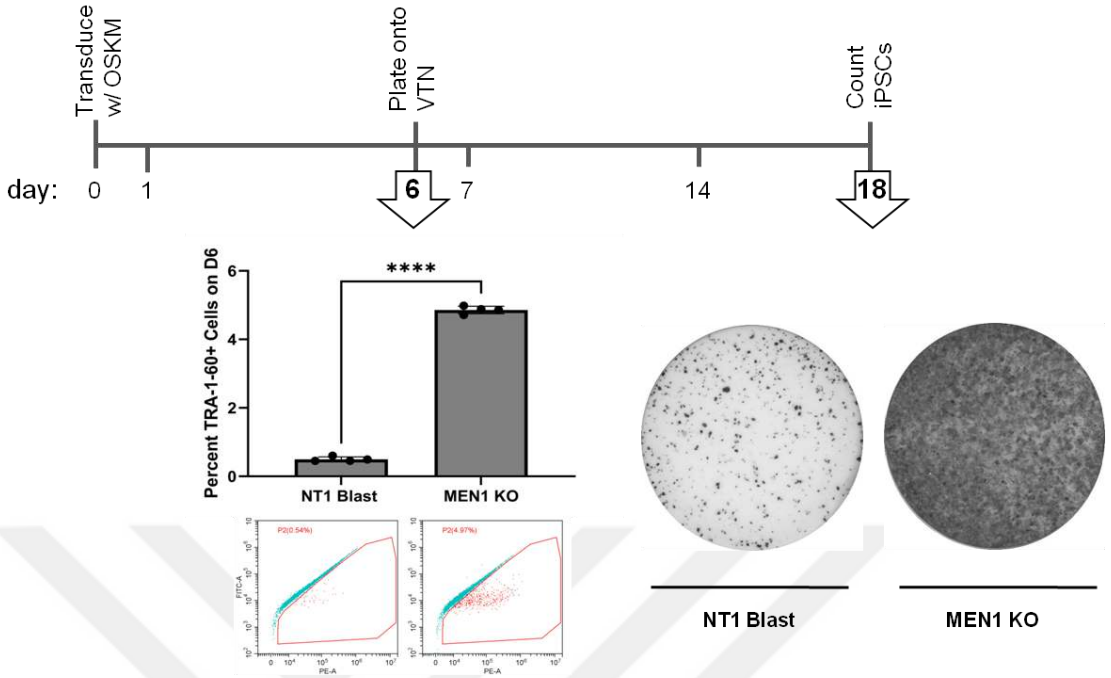

Figure 3.6. Flow cytometry analysis performed on Day 6 after OSKM induction. The representative well images are TRA-1-60+ cells at the end of reprogramming. n=4 independent experiments were performed. Error bars represent error of mean. Two-tailed t-test analysis was performed. **** stands for p≤0.0001. Well images are TRA-1-60 staining results at the end of reprogramming.

Next, we performed bulk RNA sequencing 6 days after the OSKM induction and without OSKM induction to determine the transcriptional changes that take place during reprogramming after the inhibition and depletion of MENIN. The transcriptional profiles were mapped using the principal component analysis (Figure 3.7).

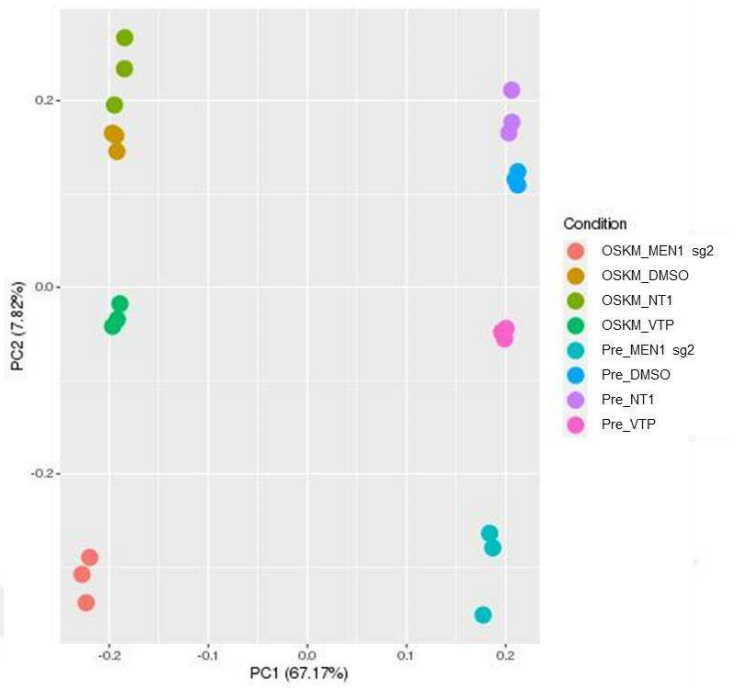

Figure 3.7. Principal component analysis of the different samples.

To determine effects of MENIN inhibition and depletion on fibroblasts, we performed RNA sequencing with samples that were not transduced with OSKM. Then, we performed gene ontology (GO) analysis with the genes that were upregulated and downregulated (Figure 3.8, Figure 3.9, Figure 3.10 and Figure 3.11). Additionally, we performed GO analysis to determine the transcriptional changes that take place in DMSO-treated and NT1 Blast fibroblasts after the OSKM induction (Figure 3.12 and Figure 3.13).

Figure 3.8. Upregulated genes after 6 days of VTP treatment under pre-OSKM conditions.

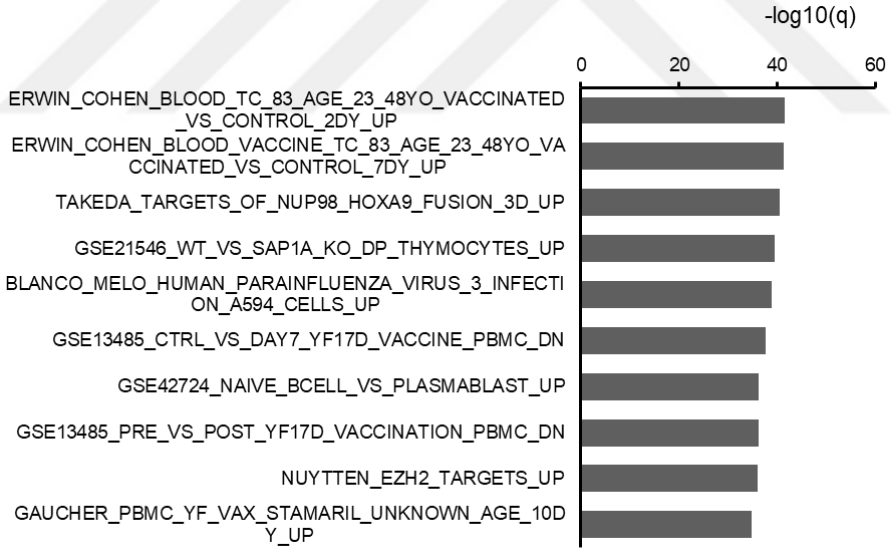

Figure 3.9. Downregulated genes after 6 days VTP treatment under pre-OSKM conditions.

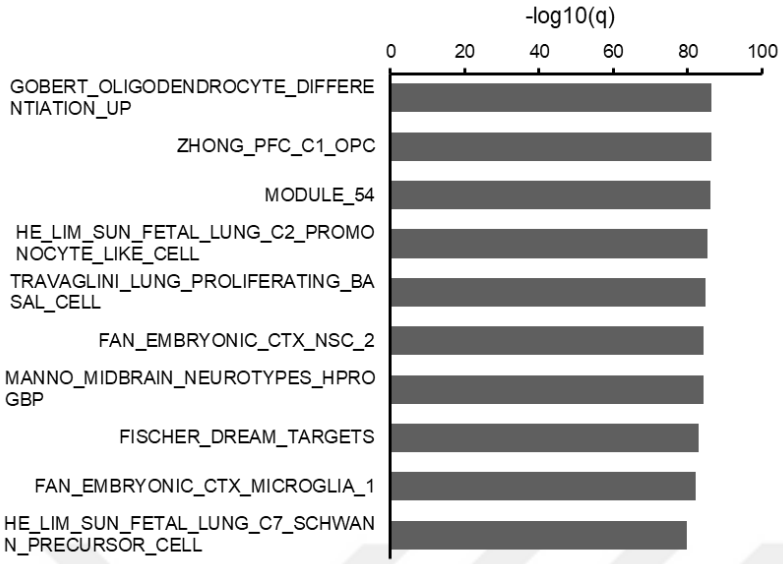

Figure 3.10. Upregulated genes after MENIN depletion under pre-OSKM conditions.

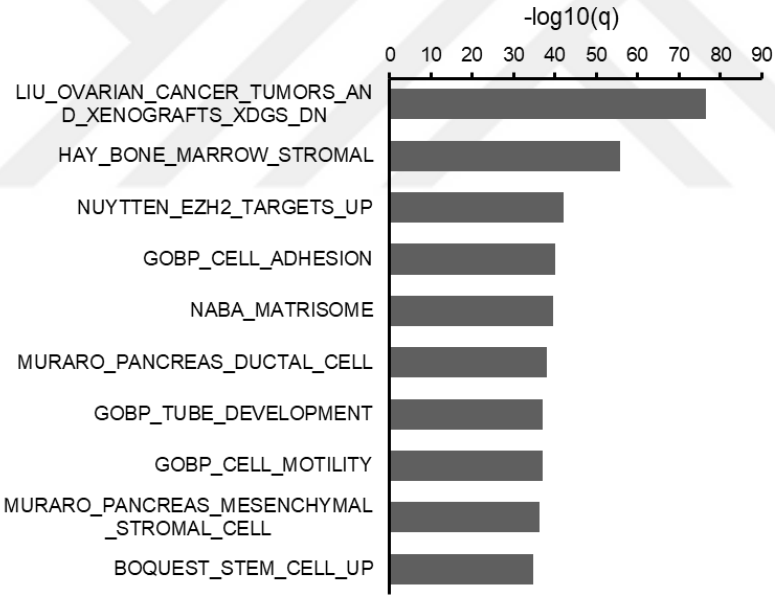

Figure 3.11. Downregulated genes after MENIN depletion under pre-OSKM conditions.

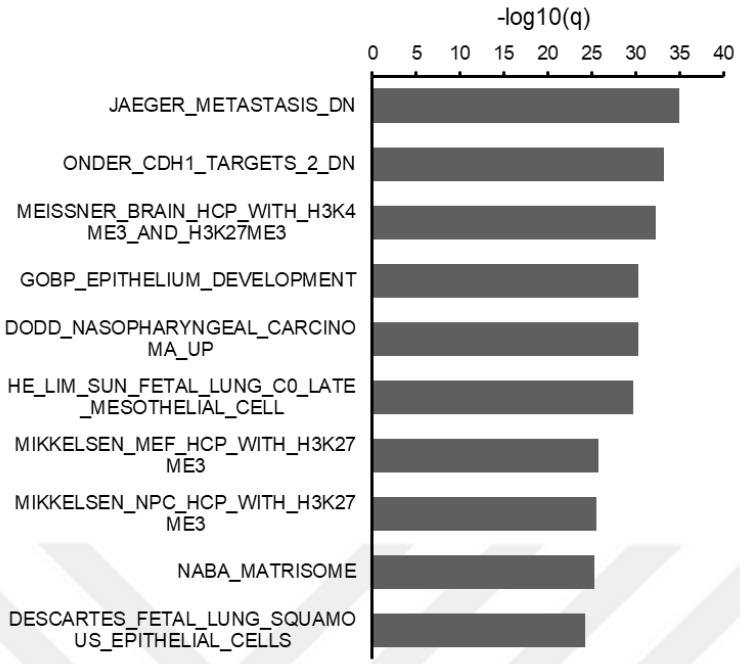

Figure 3.12. The upregulated genes after the OSKM induction in DMSO treated fibroblasts.

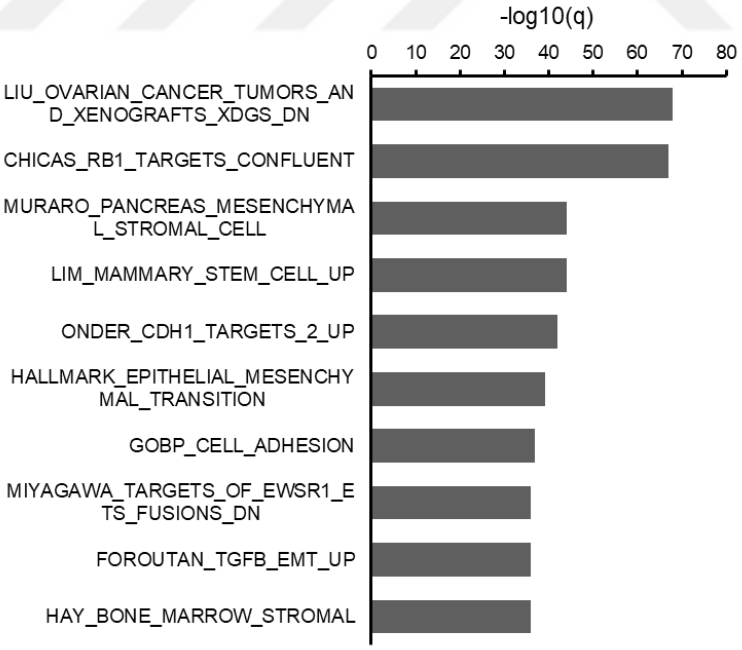

Figure 3.13. The downregulated genes after the OSKM induction in DMSO treated fibroblasts.

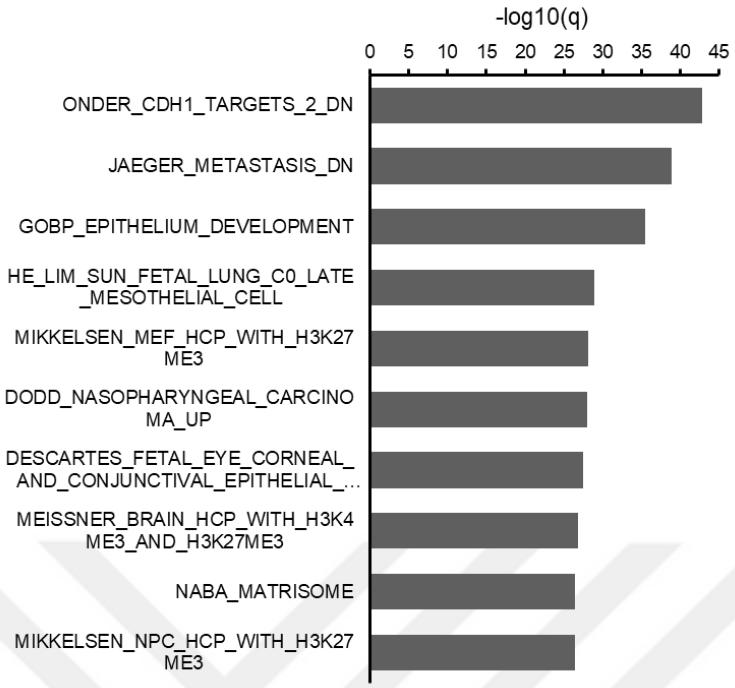

Figure 3.14. The upregulated genes after the OSKM induction in NT1 Blast fibroblasts.

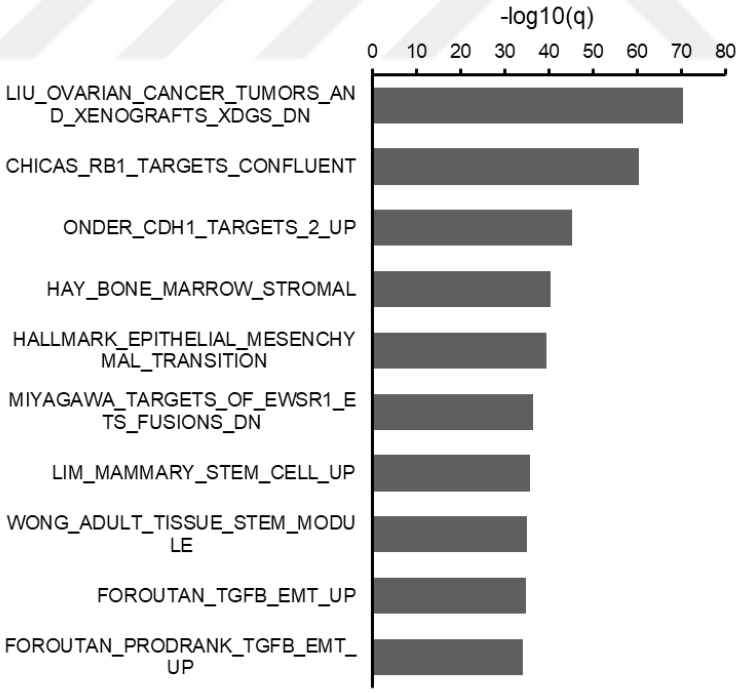

Figure 3.15. The downregulated genes after the OSKM induction in NT1 Blast fibroblasts.

One possible explanation for the robust induction of the pluripotency was that MENIN inhibition and depletion leads to derepression of the pluripotency circuitry even without the OSKM factors. To test that, we have cross-referenced the genes upregulated in MENIN inhibition and depletion conditions with the pluripotency related genes. While there were no genes that were upregulated in both the MENIN inhibition and depletion, 7 pluripotency related genes were upregulated in MENIN depleted cells under pre-OSKM conditions. To our surprise, we found CDH3, a surface marker that characterize late stage reprogramming (Pomeroy et al., 2016), to be one of the 7 upregulated genes (Figure 3.16). Interestingly, we observed that, despite the lack of OSKM induction a number of fibroblast-related genes were downregulated. This suggests that MENIN might be involved in maintaining the expression of fibroblast-related genes which safeguard the fibroblast cell identity.

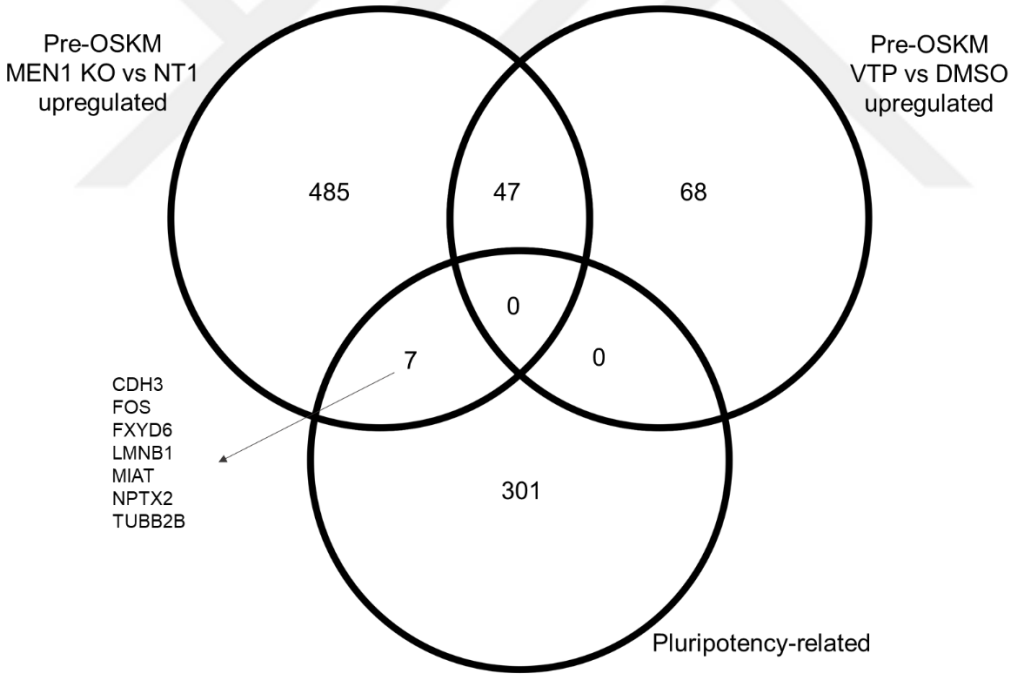

Figure 3.16. Mutually upregulated genes related to pluripotency between VTP-treated and MEN1 KO cells under pre-OSKM conditions.

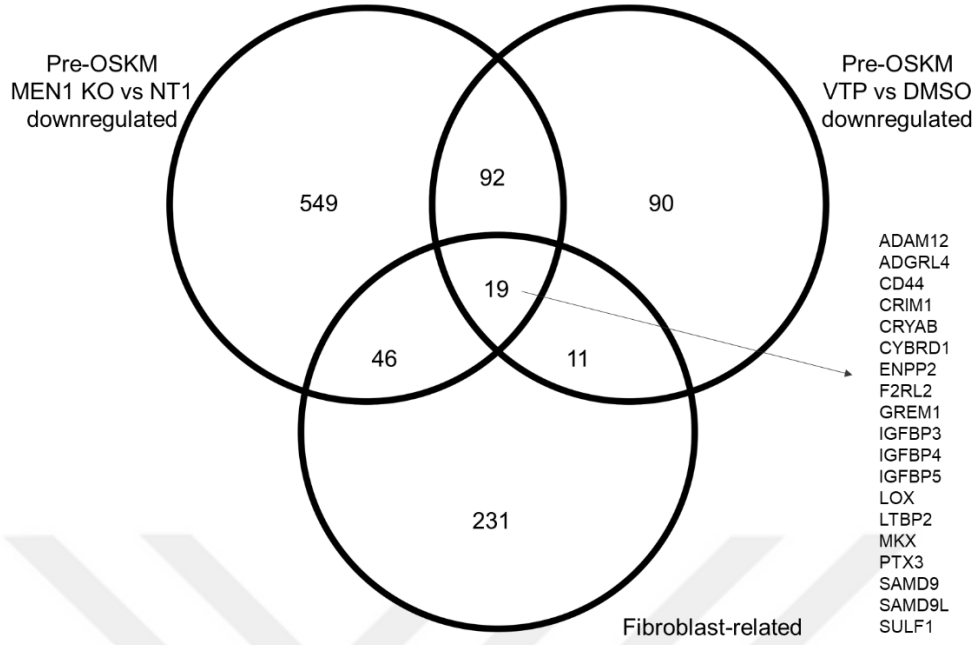

Figure 3.17. Mutually downregulated genes related to fibroblast identity between VTP-treated and MEN1 KO cells under pre-OSKM conditions.

Additionally, we performed gene ontology analysis to determine gene sets that are differentially upregulated and downregulated after MENIN inhibition under OSKM conditions (Figure 3.18, Figure 3.19) and depletion (Figure 3.20, Figure 3.21).

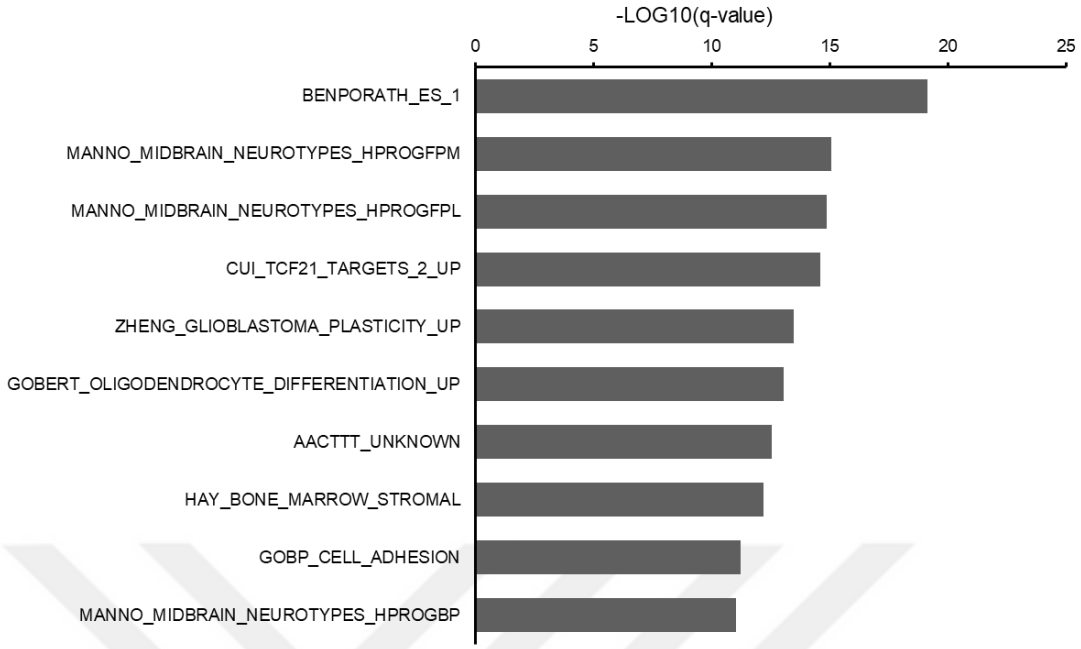

Figure 3.18. Upregulated genes after the VTP treatment at day 6 of reprogramming compared to DMSO.

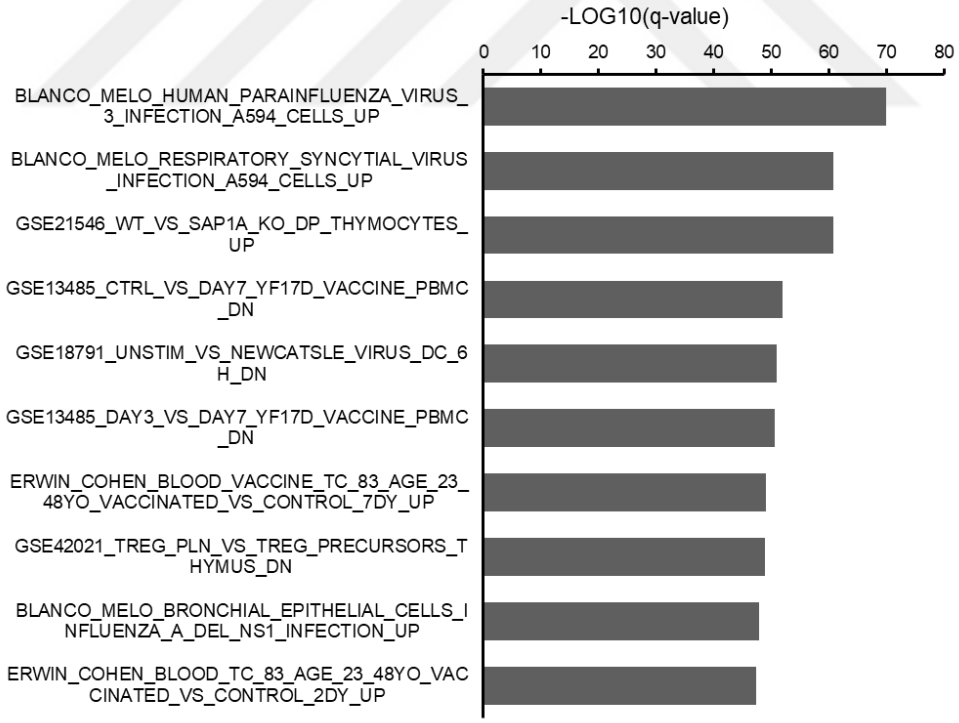

Figure 3.19. Downregulated genes after the VTP treatment at day 6 of reprogramming compared to DMSO.

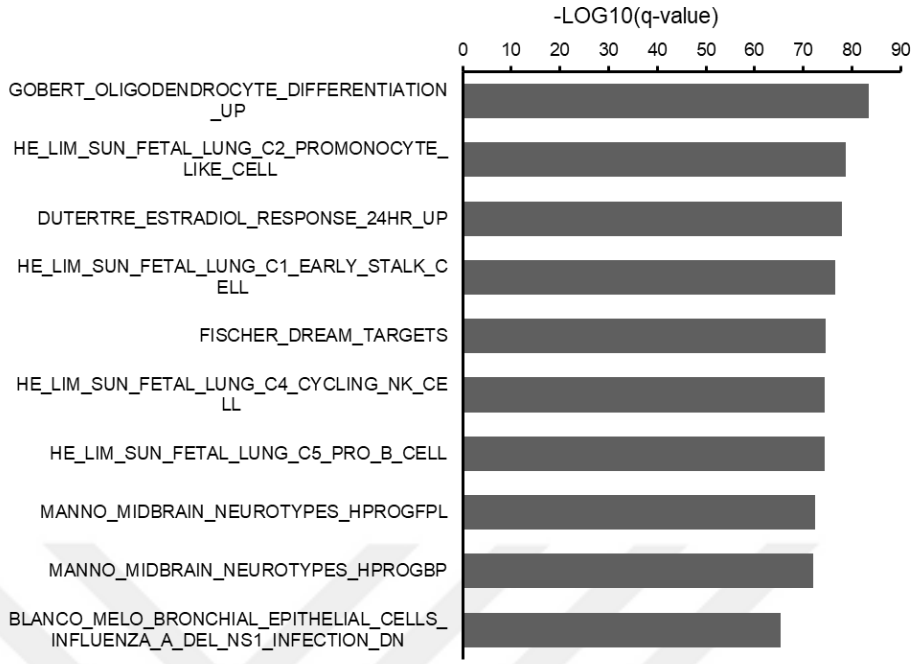

Figure 3.20. Upregulated genes after MEN1 depletion at day 6 reprogramming compared to NT1.

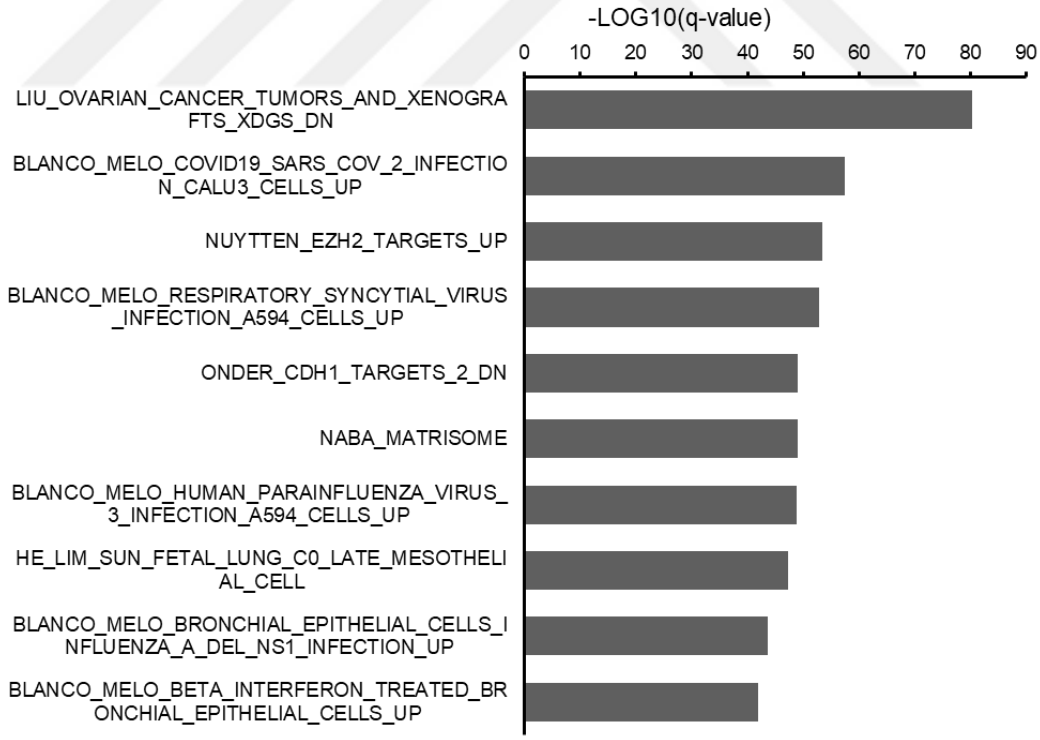

Figure 3.21. Downregulated genes after MEN1 depletion at day 6 reprogramming compared to NT1.

We, next, determined the mutually upregulated pluripotency-related genes and downregulated fibroblast-related genes between MEN1 KO and VTP treatment (Figure 3.22, Figure 3.23) during reprogramming. We aimed to test if MENIN performs its barrier function via repressing pluripotency genes directly. We also wanted to test if MENIN retains the fibroblast cell identity which works against the acquisition of pluripotent state which has been suggested to be a mechanism of action in reprogramming (Michlits et al., 2017). Interestingly, we observed the upregulation of pluripotency markers (Figure 3.22), such as NANOG, SALL4 and DNMT3B, that are usually expressed late in the reprogramming process (Buganim et al., 2013). Interestingly, we observed the upregulation of DPPA4 in the contexts of MENIN inhibition and depletion (Figure 3.22). DPPA4 is a marker associated with naïve pluripotency (Osnato et al., 2021).

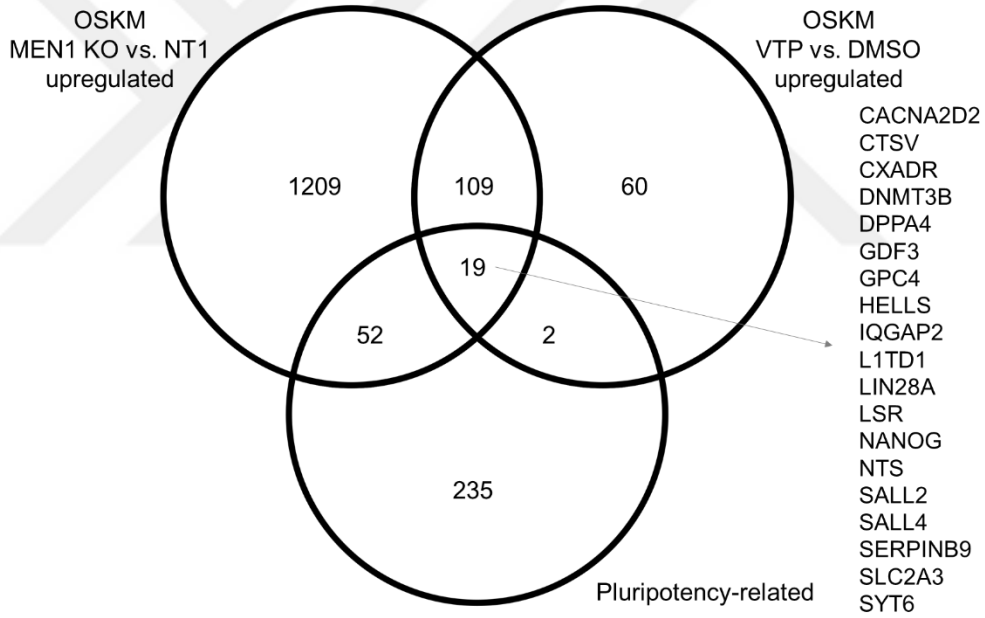

Figure 3.22. Mutually upregulated genes related to pluripotency between VTP-treated and MEN1 KO cells after OSKM induction.

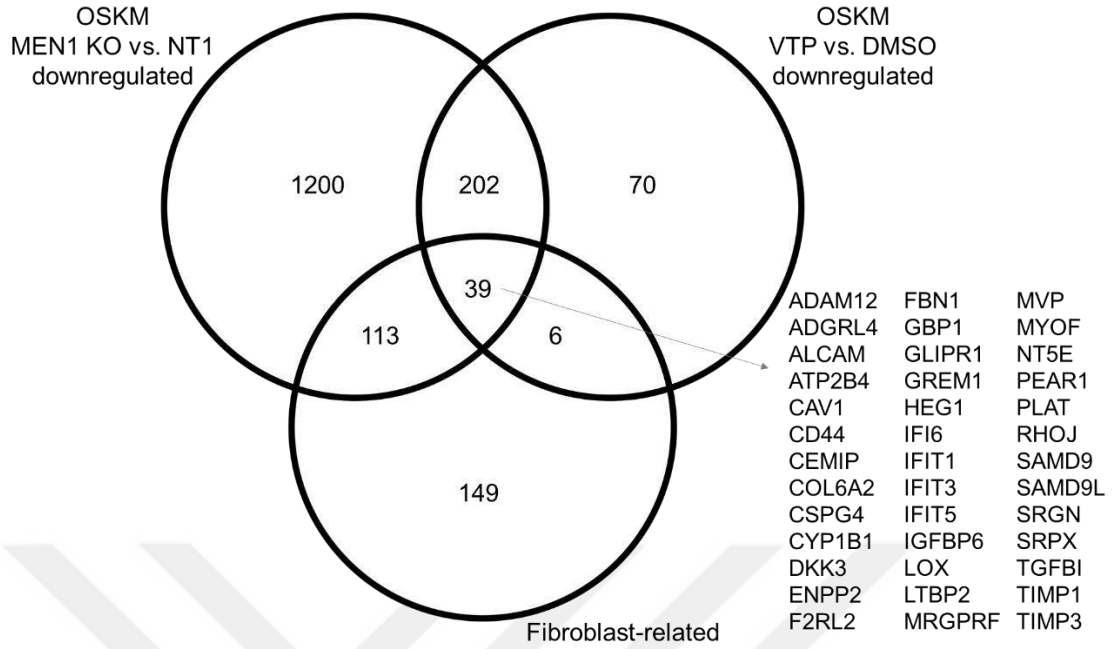

Figure 3.23. Mutually downregulated genes related to fibroblast identity between VTP-treated and MEN1 KO cells after OSKM induction.

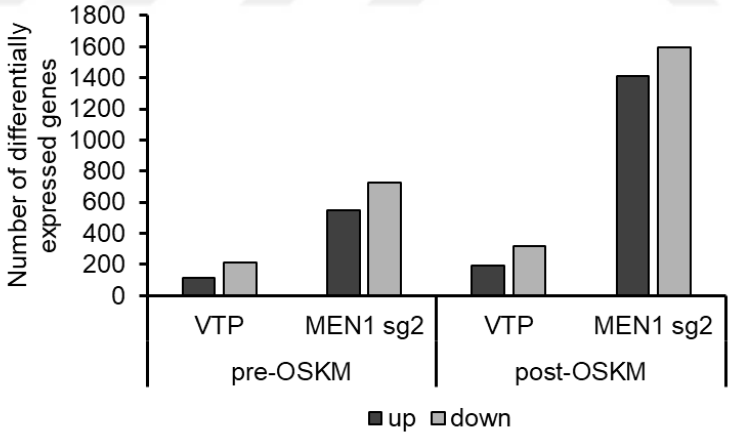

Figure 3.24. The number of differentially expressed genes compared to their respective controls DMSO and NT1 Blast under post-OSKM and pre-OSKM conditions.

Overall, RNA sequencing data shows that it is possible that MENIN represses the pluripotency genes possibly via maintaining the expression of certain fibroblast-specific genes. Therefore, in the absence of MENIN activity, OSKM factors resets the somatic

cell identity in much more efficient manner which facilitates the awakening of the pluripotency network resulting in robust increase in the reprogramming efficiency.

To test which interaction partners or MENIN complexes act as barriers to reprogramming, we set up genetic rescue experiments using mutant MEN1 cDNAs known to be deficient in differential binding to MLL1 and PSIP1. Wild type and point mutant MEN1 plasmids were overexpressed in MEN1 knockout fibroblasts. The point mutants were chosen from literature studying the identified mutations in patients suffering conditions due to the defects in MENIN's function (Table 3.1).

Table 3.1. Interaction and MLL1-dependent transcription capabilities of the chosen MEN1 point mutants. * represents impaired association (Dreijerink et al., 2022; Yokoyama & Cleary, 2008)

	MLL Binding	PSIP1 Binding	MLL Transcription
Menin	+	+	+
P12L	+	-	-
T344R	-*	-	Not determined.
H139D	-	-	Not determined.
A242V	-*	-*	Not determined.
E255K	-	Not determined.	Not determined.

Overexpression of mutant Menin proteins in Men1 KO cells were confirmed with Western blotting (Figure 3.25). Cells infected with the T344R mutant vector did not exhibit any MENIN expression at the protein level. This is likely due to the reduced stability of this mutant which has been reported previously (Canaff et al., 2012).

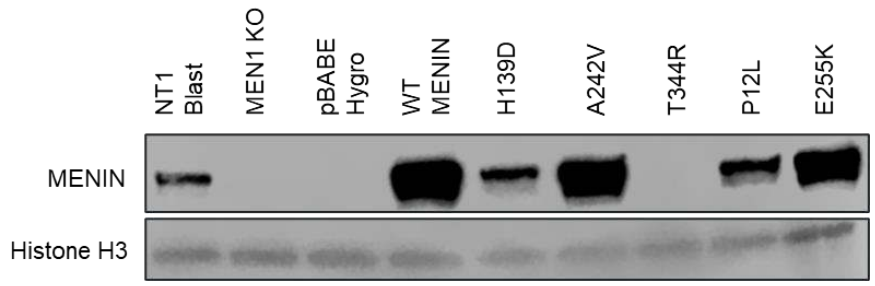

Figure 3.25. Western blot image showing MENIN protein levels after MEN1 overexpression in MEN1-targeting gRNA expressing fibroblasts. H3 Total was used as a loading control.

Following confirmation of MENIN expression, cells were transduced with OSKM and the ability of the various cDNAs to rescue the increased reprogramming phenotype was examined. As expected, overexpression of WT-MEN1 rescued the MEN1 KO phenotype, resulting robust suppression of reprogramming (Fig 3.26). In line with the Western blot data, T344R failed to rescue the phenotype. Interestingly, P12L, A242V and E255K mutants partially reversed the increased reprogramming efficiency (Figure 3.26).

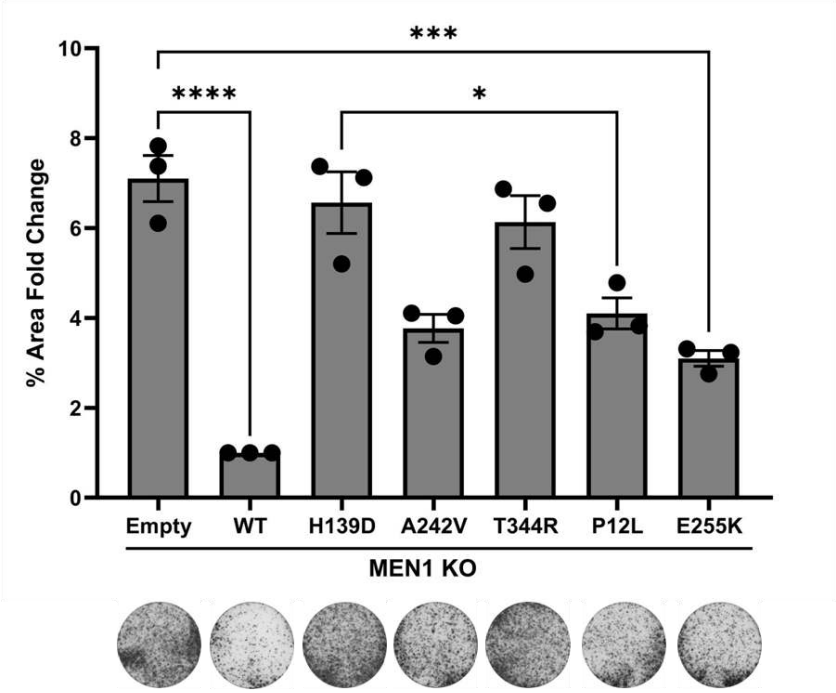

Figure 3.26. Fold change in percent area upon MEN1 overexpression in MEN1 KO background. Error bars indicate the error of mean. n=3, independent experiments were

performed. * stands for p≤0.05, ** stands for p≤0.01, *** stands for p≤0.001, **** stands for p≤0.0001.

MEN1 P12L point mutation has been shown to be incapable of inducing MLL1-dependent transcription despite maintaining the ability to interact with MLL1. This loss of MLL1-dependent transcription occurs due to the lack of PSIP1 binding which is another interaction partner of MLL1-MENIN complex (Yokoyama & Cleary, 2008). P12L rescue suggests that the barrier function of the MLL-MENIN complex might be related to the non-catalytic activity of MENIN-MLL1. Moreover, E255K has recently been shown to be a mutant that lacks MLL1 interaction completely while retaining a modest interaction capability with JUND (Dreijerink et al., 2022). This suggests that barrier function of MENIN extends beyond its interaction with MLL1 possibly to JUND.

Next, we tested if MEN1 deletion can enable reprogramming with only OCT4 and SOX2. While there was a small number of colonies in the NT1 control wells, MEN1 KO cells could be reprogrammed successfully (Figure 3.27). This demonstrates that MENIN is a strong repressor of reprogramming.

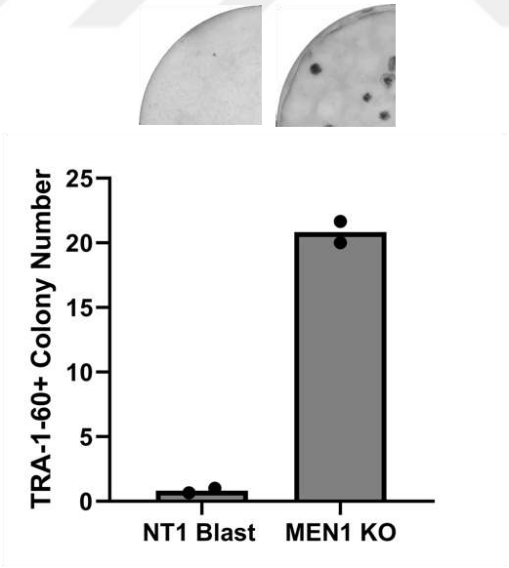

Figure 3.27. TRA-1-60 colony numbers after OS reprogramming. n=2, independent experiments were performed.

3.4 MENIN as a barrier in the context of DOT1L inhibition

Since a recent paper reported that MENIN is a "reader" of the H3K79me2 mark (Lin et al., 2023), we decided to investigate if the enhanced reprogramming efficiency can be explained by this reader function of MENIN. It has been well established that DOT1L inhibition leads to depletion of the H3K79 methylation mark and increases the efficiency of reprogramming. Therefore, we decided to combine DOT1L inhibition with MENIN inhibition and deletion. We observed that, when the DOT1L inhibitor is combined with VTP, it doesn't lead to an additive increase in the reprogramming efficiency (Figure 3.28).

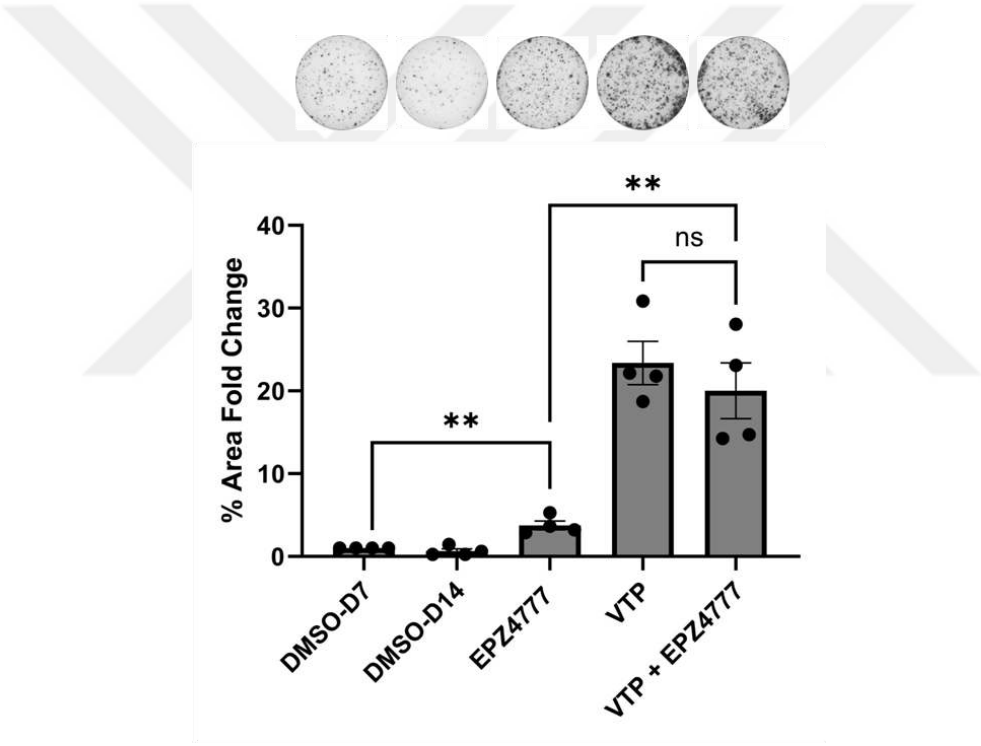

Figure 3.28. Fold change in percent area of TRA-1-60+ colonies after inhibitor treatments. VTP treatment was performed during the first two weeks of reprogramming at a concentration of 1 μM. EPZ4777 treatment was performed during the first week of reprogramming at a concentration of 3 μM. Error bars indicate the error of mean. n=4, independent experiments were performed. * stands for $p \leq 0.05$, ** stands for $p \leq 0.01$,

To further validate our results, we have utilized the DOT1L inhibitor, EPZ4777 in NT1 and MEN1 gRNA expression background. We again observed that DOT1L

inhibition does not lead to further enhancement of the reprogramming efficiency when combined with the MENIN depletion (Figure 3.29).

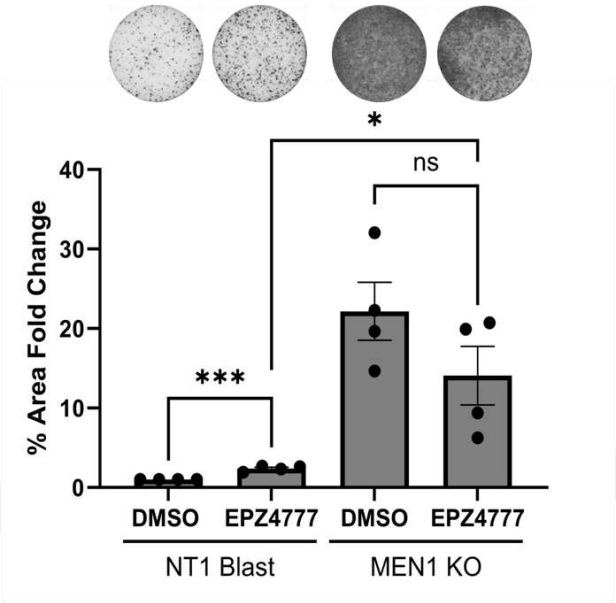

Figure 3.29. Fold change in percent area of TRA-1-60+ colonies after EPZ4777 treatment of NT1 and MEN1 targeting gRNA expressing fibroblasts. Error bars indicate the error of mean. n=4, independent experiments were performed. * p≤0.05, *** p≤0.001.

3.5 MLL1-MENIN Complex and MENIN act as a barrier in naive reprogramming

Next, we tested whether the enhanced efficiency with the MENIN inhibition paradigm was also applicable for reprogramming to induced naive pluripotent stem cells.

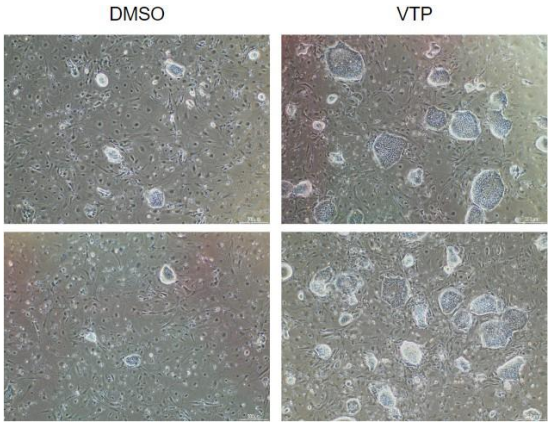

Figure 3.30. Brightfield images of DMSO and VTP treated wells after naive reprogramming.

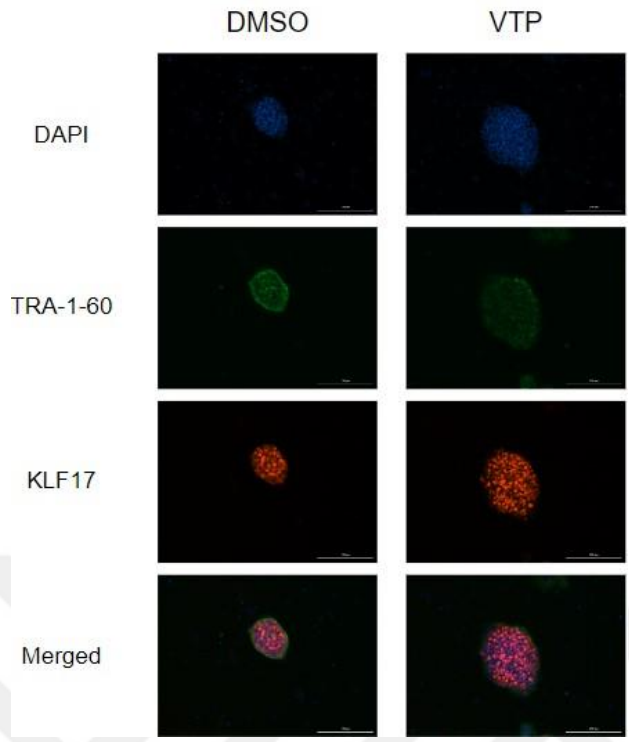

Figure 3.31. Immunofluorescent images of DMSO and VTP-treated wells stained for TRA-1-60 and KLF17 after naive reprogramming. DAPI staining was performed to visualize the nuclei. Scale bars denote 200 μm.

We observed that VTP treatment in the first 2 weeks of reprogramming leads to a dramatic increase of near 5-fold in the number of naive PSC colonies (characterized by KLF17 staining) formed at the end of reprogramming (Figure 3.30, Figure 3.31 and Figure 3.32). We observed that knocking out MEN1 gene induces significantly higher enhancement compared to the inhibitor treatment which is also observed in the primed reprogramming (Figure 3.33, Figure 3.34, Figure 3.35).

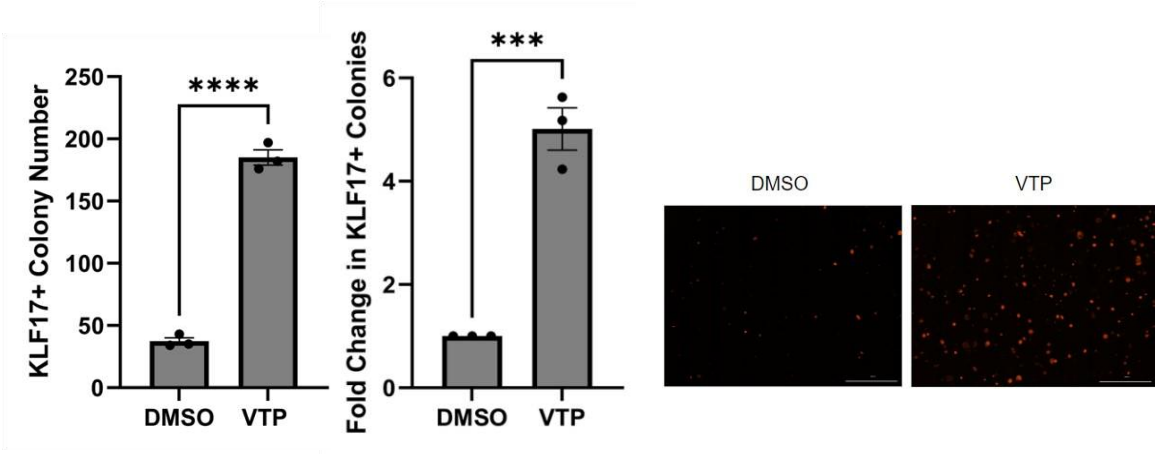

Figure 3.32. The number and the fold change of KLF17+ colonies at the end of reprogramming after 1 µM VTP treatment during the first two weeks of reprogramming. Error bars indicate the error of mean. n=4, independent experiments were performed. * stands for p≤0.05, ** stands for p≤0.01, *** stands for p≤0.001, **** stands for p≤0.0001. Scale bars denote 3000 µm.

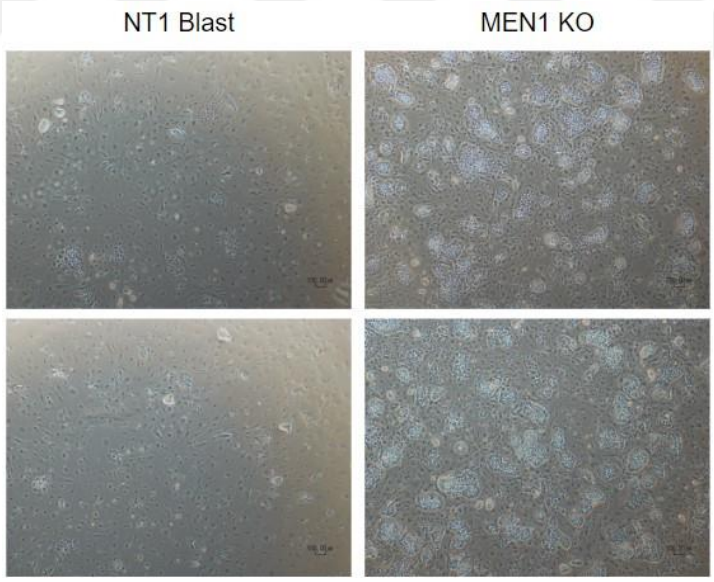

Figure 3.33. Brightfield images of NT1 and MEN1 targeting gRNA expressing fibroblasts after naive reprogramming. Scale bars denote 100 µm.

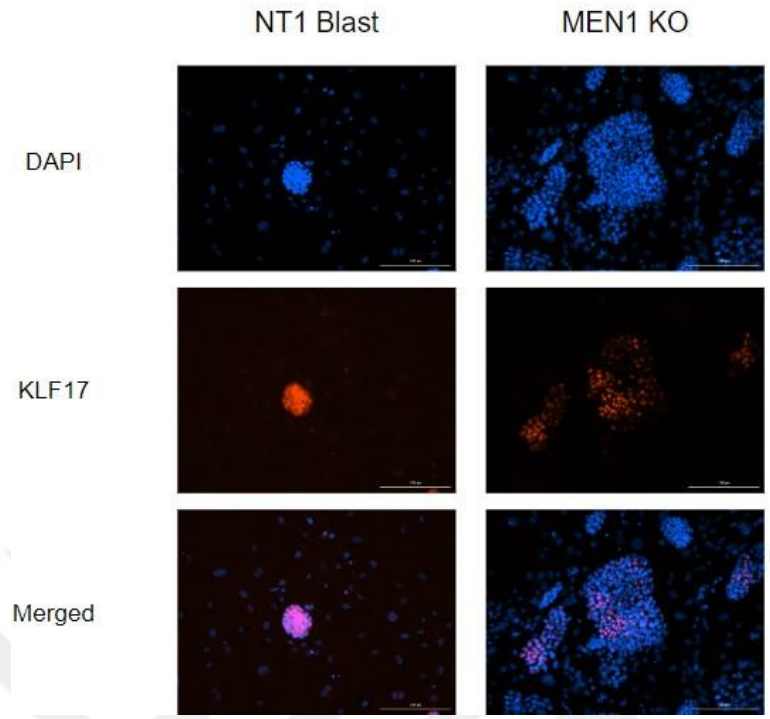

Figure 3.34. Immunofluorescent images of NT1 and MEN1 targeting gRNA expressing fibroblasts stained for KLF17 after naive reprogramming. DAPI staining was performed to visualize the nuclei. Scale bars denote 200 µm.

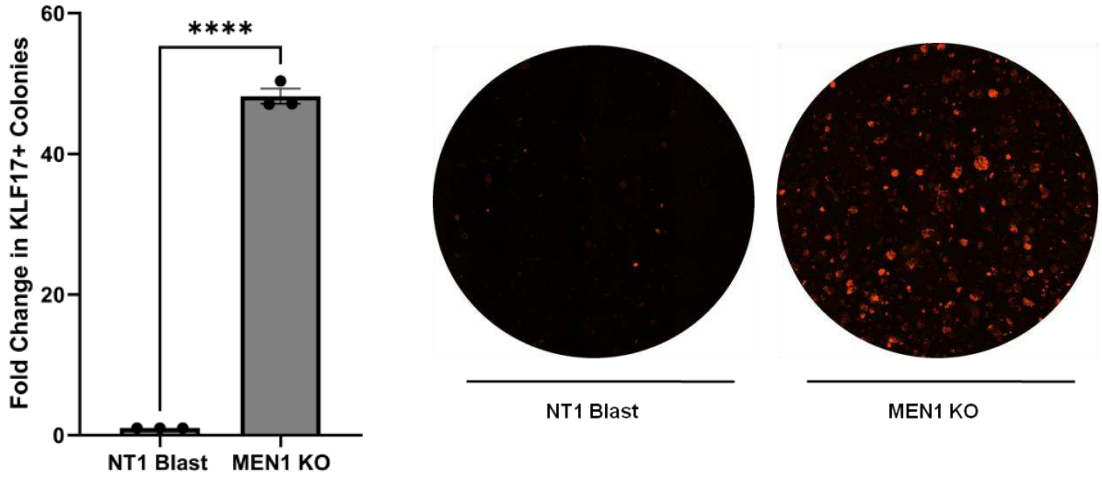

Figure 3.35. The fold change of KLF17+ colonies at the end of naive reprogramming of NT1 and MEN1 targeting gRNA expressing fibroblasts. Error bars indicate the error of mean. n=4, independent experiments were performed. * stands for p≤0.05, ** stands for p≤0.01, *** stands for p≤0.001, **** stands for p≤0.0001.

3.6 Inhibition of MENIN-MLL1 complex enhances the acquisition of an enhanced naive state

MLL1 has previously been implicated in the repression of pluripotency by upregulating the commitment-associated genes in mice (Zhang et al., 2016). Considering that this might be the mechanism of its barrier function, we aimed to test the same paradigm in human PSCs. To do that, we optimized a recently published method (Bayerl et al., 2021) to acquire human naive pluripotent stem cells. Using this previously published protocol, we converted two different PSC lines (H9 ESCs and NO#2 iPSCs) to naive PSCs using the HENSM-ACT media condition. The acquired naive cells were characterized via RT-qPCR (Figure 3.37, Figure 3.39) and immunofluorescence staining for pluripotency markers such as KLF17, OCT4 and NLRP2 (Figure 3.40).

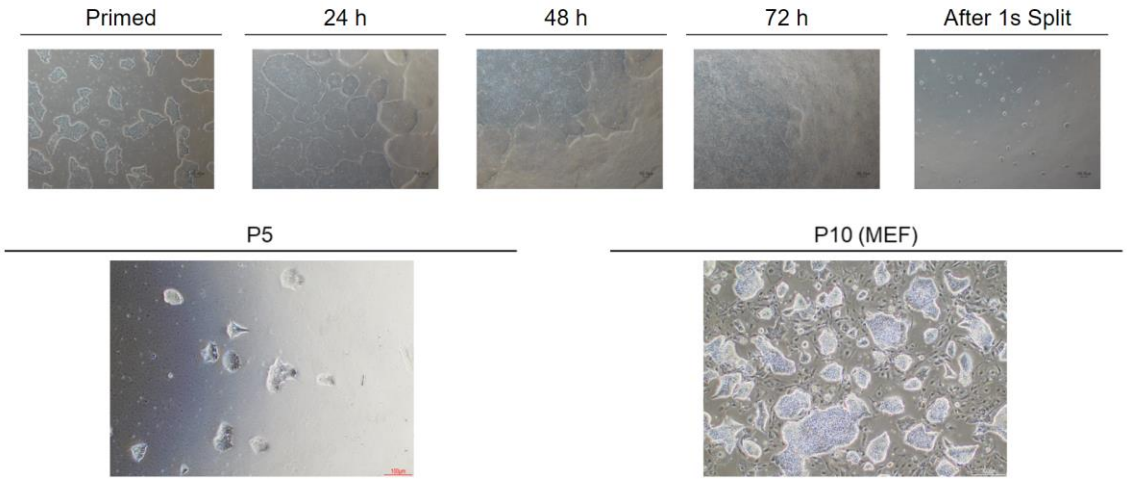

Figure 3.36. Brightfield images from different time points of H9 ESCs naive conversion with HENSM-ACT media conditions. Scale bars denote 100 µm or 300 µm.

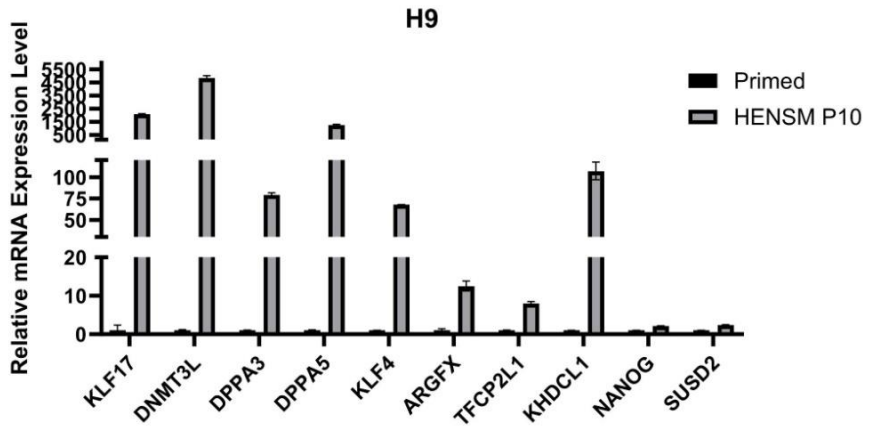

Figure 3.37. Gene expression levels of H9 ESCs after naive conversion for naive pluripotency associated markers. Normalization was performed with respect to the primed cells. GAPDH was used as the housekeeping gene.

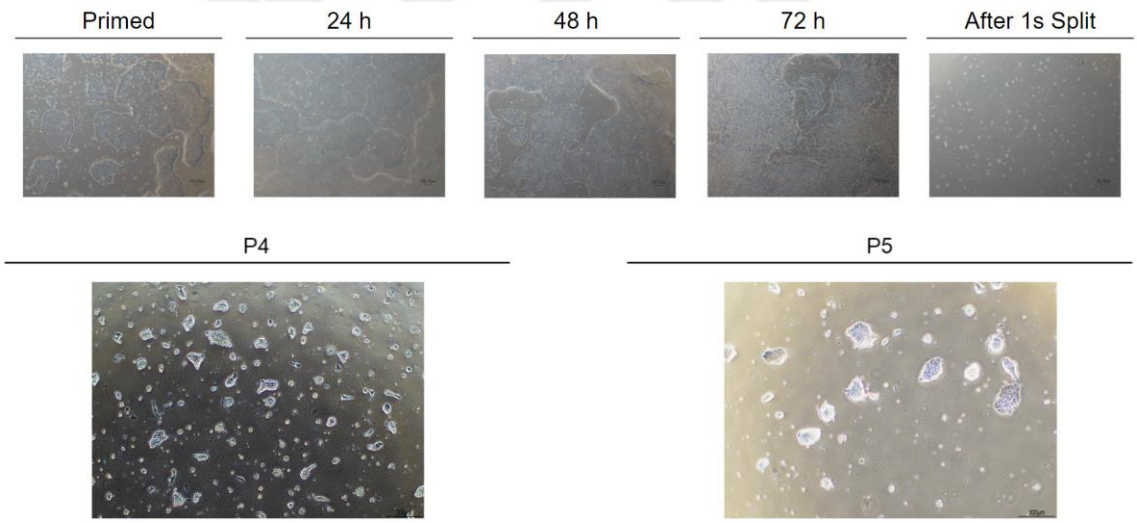

Figure 3.38. Brightfield images from different time points of NO #2 iPSCs naive conversion with HENSM-ACT media conditions. Scale bars denote 100 µm or 300 µm.

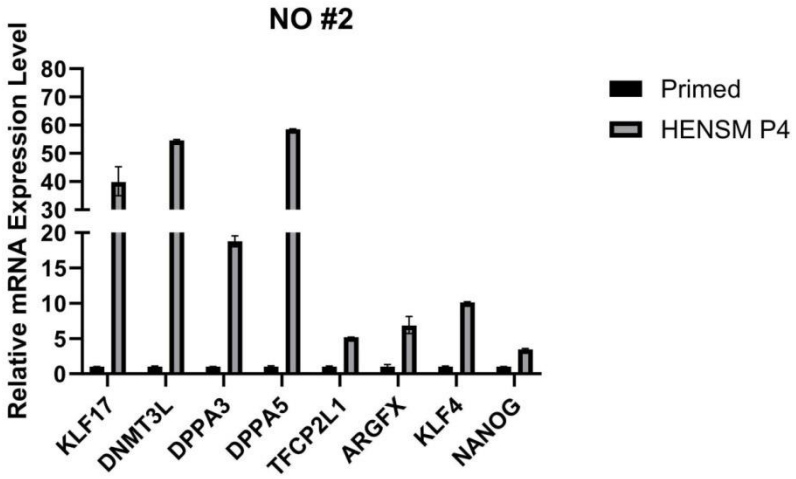

Figure 3.39. Gene expression levels of NO #2 iPSCs after naive conversion for naive pluripotency associated markers. Normalization was performed with respect to the primed cells.

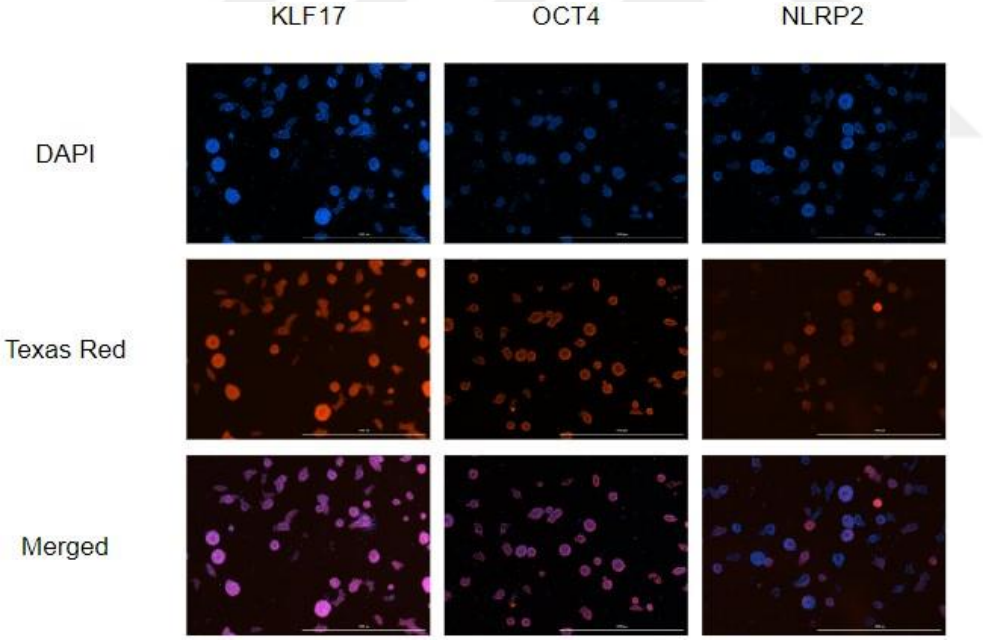

Figure 3.40. Immunofluorescent images of NO#2 iPSCs after naive conversion. Staining was performed for KLF17, NLRP2 and OCT4. DAPI staining was performed to visualize the nuclei.

RT-qPCR results showed that HENSM-ACT conditions induced robust upregulation in gene expression levels of a number of naive pluripotency associated markers such as KLF17, DNMT3L, DPPA3, DPPA5 and KLF4. To confirm the naive state on the protein level, immunofluorescence staining was performed for KLF17, OCT4 and NLRP2. After confirming that HENSM-ACT conditions can be used for converting different cell lines to naive PSCs, we employed a reporter cell line WIBR3 Delta PE OCT4 GFP cell line that has been utilized previously for screening naive cell conversion (Theunissen et al., 2014). This line specifically gives GFP signal when cells start expressing OCT4 via its distal enhancer element which is a hallmark of naive pluripotency. Using this line, we aimed to determine the effects of MLL1-MENIN inhibition on resetting primed PSCs to a naive state. Flow cytometry experiments showed that when VTP was combined with the HENSM-ACT media condition, it increased the percentage of GFP-positive cells nearly 1.5-fold (Figure 3.41).

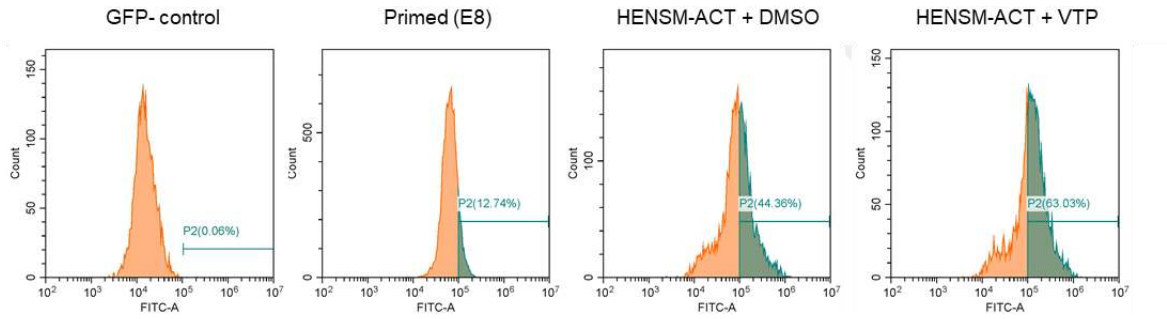

Figure 3.41. Flow cytometry analysis was performed to determine the levels of GFP signals after 3 passages with naive conversion media supplemented with DMSO or VTP. n=1, experiment was performed.

To confirm our findings, qPCR was performed to measure the expression level of naive-related markers. Compared to the DMSO control, VTP-treated cells showed greater levels of upregulation for genes associated with naive pluripotency such as KLF17, DNMT3L and KLF4 (Figure 3.42).

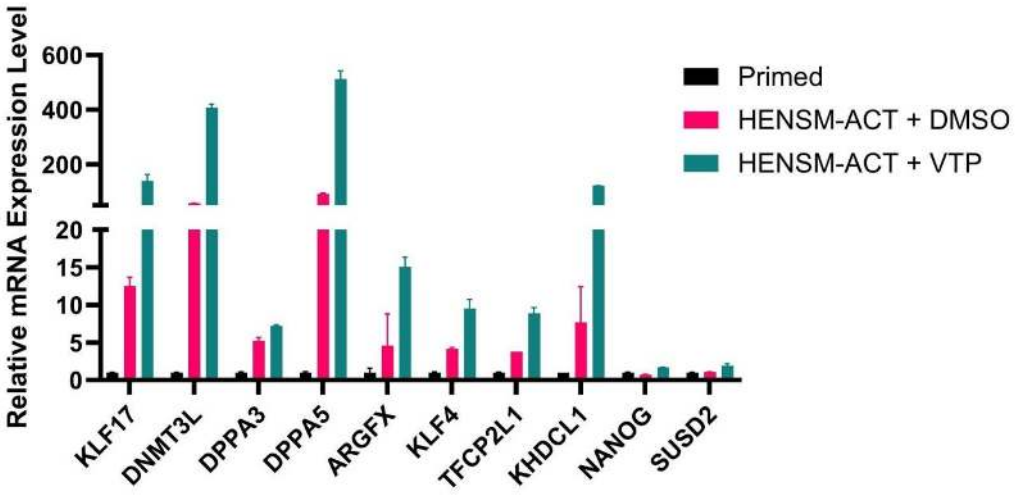

Figure 3.42. Gene expression levels of the WIBR3 Delta PE OCT4 GFP cells for naive pluripotency associated markers after naive conversion with DMSO and VTP. Normalization was performed with respect to the primed cells. VTP treatment was performed during the first three passages with a concentration of 1 μM.

Next, we aimed to test if this phenotype is specific to the WIBR3 Delta PE OCT4 GFP cell line. For this purpose, we performed the same procedure with the WIBR3 OCT4 GFP cell line. After 2 passages in the HENSM-ACT + VTP media, cells showed greater levels of gene expression levels for naive pluripotency related markers (Figure 3.43).

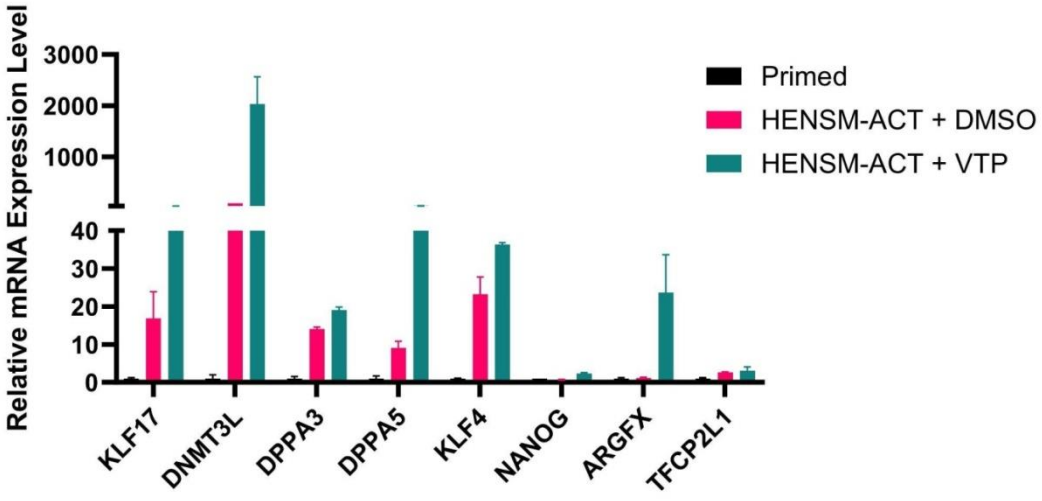

Figure 3.43. Gene expression levels of the WIBR3 OCT4 GFP cells for naive pluripotency associated markers after naive conversion with DMSO and VTP. VTP treatment was performed during the first two passages with a concentration of 1 μM.

Next, we asked if the enhancement effect is specific to the resetting stage. To examine whether VTP treatment accelerates the acquisition of naive pluripotency or boost the expression of naïve markers, we treated an already naive cell line with VTP for 2 passages. Using RT-qPCR, I observed that there was nearly 2-fold increase in key naive pluripotency markers such as KLF17 and DNMT3L. Expression levels of other markers such as DPPA3 and DPPA5 remained unchanged (Figure 3.44). These data suggests that Menin inhibition boosts the expression level of a subset of naïve genes in naive cells even after two passages of treatment.

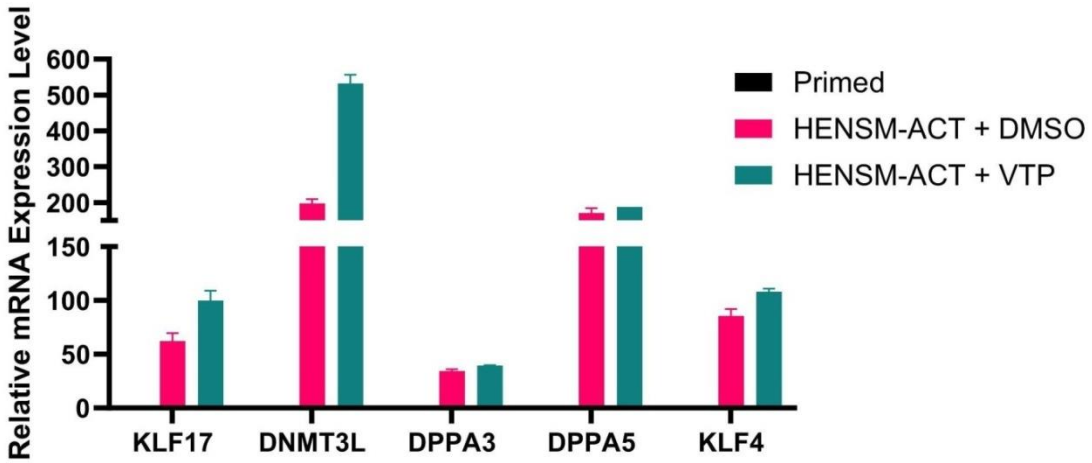

Figure 3.44. Gene expression levels of the naive NO #2 iPSCs after 2 passages of treatment with DMSO or VTP. Normalization was performed with respect to the primed cells. VTP treatment was performed during two passages with a concentration of 1 μM.

To test if Menin inhibitors can be used as an additional component for the acquisition and maintenance of human naïve PSCs, WIBR3 OCT4 GFP cell line was grown in the presence of HENSM-ACT + VTP for 10 passages. At the end of 10 passages, the cells stained positive for KLF17, OCT4 and LAMA4 which are markers for general and naive pluripotency (Figure 3.45, Figure 3.46 and Figure 3.47). These results highlight that supplementation of naive culture conditions with VTP does not induce differentiation after long term passaging.

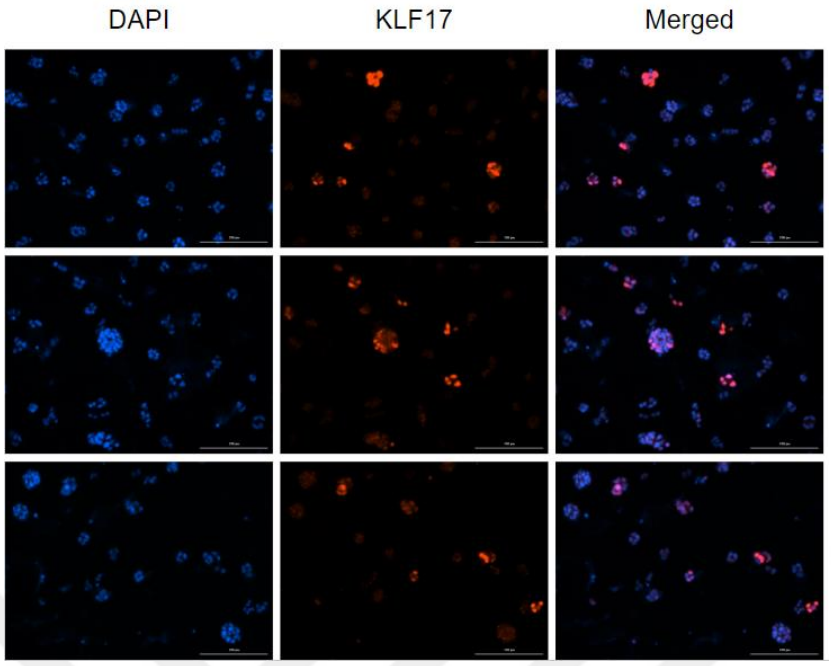

Figure 3.45. KLF17 immunofluorescence images of WIBR3 OCT4 GFP naive PSCs after treatment with HENSM-ACT + VTP media conditions for 10 passages. DAPI staining was performed to visualize the nuclei.

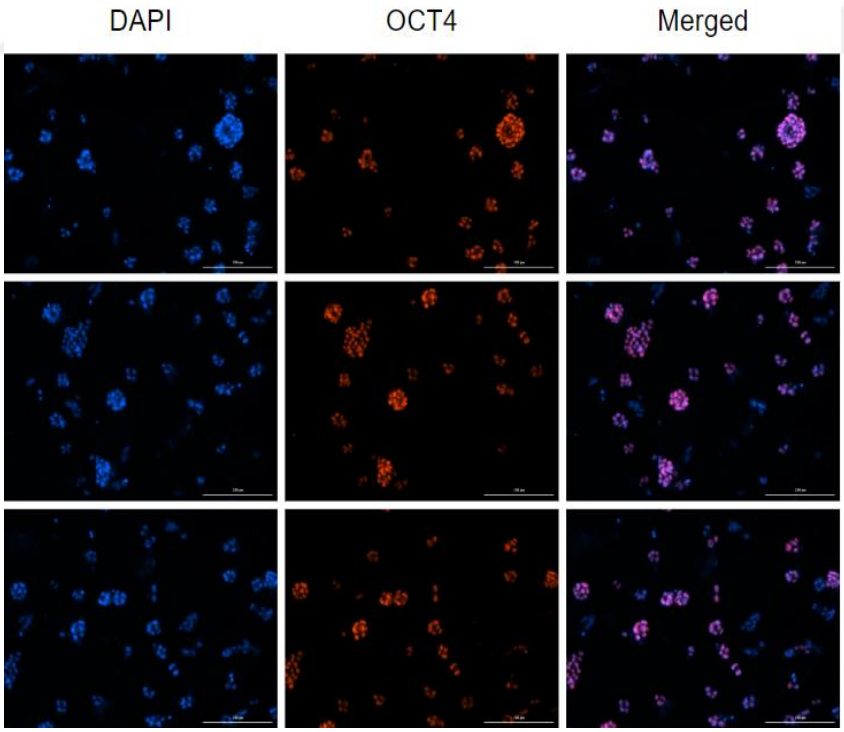

Figure 3.46. OCT4 immunofluorescence images of WIBR3 OCT4 GFP naive PSCs after treatment with HENSM-ACT + VTP media conditions for 10 passages. DAPI staining was performed to visualize the nuclei.

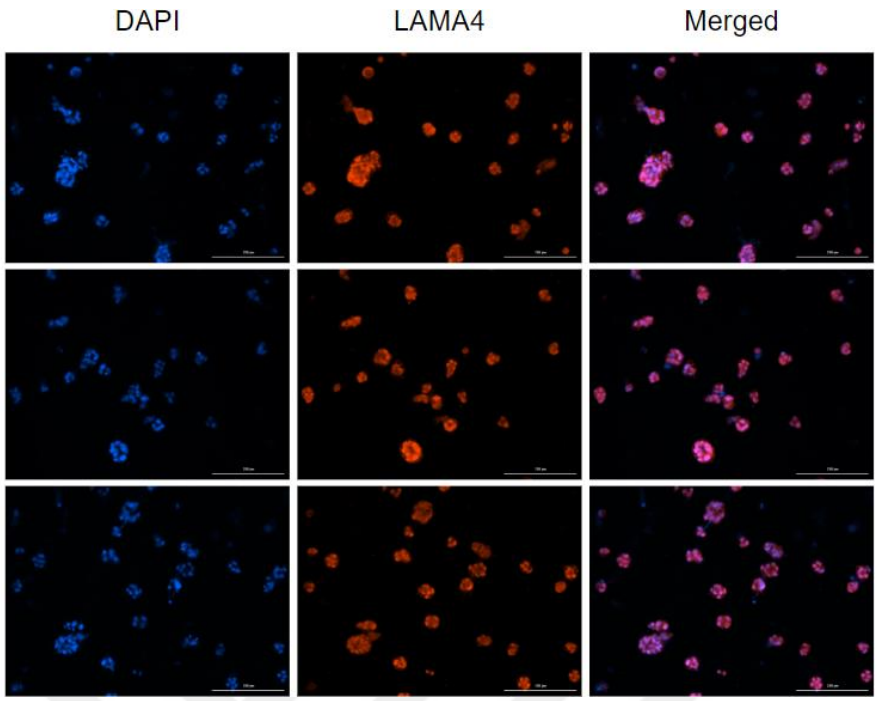

Figure 3.47. LAMA4 immunofluorescence images of WIBR3 OCT4 GFP naive PSCs after treatment with HENSM-ACT + VTP media conditions for 10 passages. DAPI staining was performed to visualize the nuclei.

Chapter 4:
DISCUSSION

In this work, I have employed pharmacological and genetic approaches to study the MLL1-MENIN complex as a barrier in somatic cell reprogramming. I showed that pharmacological inhibition of this complex with a potent inhibitor, VTP50469, leads to dramatic increases in the reprogramming. Additionally, I identified a time window and a concentration level for VTP treatment to overcome the barrier function of MLL1-MENIN complex in human somatic cell reprogramming successfully. Following that, I have confirmed my findings using genetic approaches. I have generated human fibroblast knockout cell lines and reprogrammed them. Interestingly, the increased efficiency phenotype I observed with the MEN1 knockout cell line was nearly 10-fold greater than the inhibitor treatment. For understanding the transcriptional changes that take place in inhibition and depletion of MENIN, I performed RNA sequencing. These experiments showed that, in the absence of MENIN, gene expression levels of a large set of fibroblast-related genes are downregulated in pre-OSKM and post-OSKM conditions. Additionally, I observed that MENIN inhibition and depletion leads to upregulation of late stage reprogramming markers such as NANOG and SALL4 (Buganim et al., 2013). Moreover, I employed point mutant MEN1 cDNAs to determine the protein interactions important for the barrier function of MENIN. I found that MLL1 binding of MENIN is crucial for preventing the reprogramming irrespective of the catalytic activity of MLL1. I also showed that JUND interaction may be important in mediating the barrier function of MENIN. Furthermore, I aimed to determine if DOT1L-related mechanisms are involved in the prevention of reprogramming mediated by MENIN. I observed that DOT1L inhibition does not lead to further increase in reprogramming when combined with MENIN inhibition and depletion. Interestingly, I found that MLL1-MENIN interaction prevents the acquisition of the naïve pluripotent state. I observed that combining the naïve culture conditions with VTP50469 leads to enhances the induction of the naïve pluripotent state. I have shown that long term supplementation of naïve culture conditions with VTP50469 is feasible for maintaining naïve pluripotent stem cells.

We utilized several point mutant MEN1 plasmids. While the work on identifying the transcriptional effects of these mutations is scarce, recent reports suggest that they lack interaction altogether or render MLL1 catalytically inactive. Interestingly, we

observed that H139D and P12L, two point mutants with similar levels of expression, rescued the phenotype at significantly different levels. It has previously been reported that H139D completely lacks the interaction capability with MLL1 while P12L can interact with MLL1 despite resulting in no MLL1- dependent transcription activity (Yokoyama & Cleary, 2008). This suggests that the barrier function of the MLL1-MENIN complex might be independent of the catalytic activity of MLL1 as a histone methyltransferase. Another interesting finding was regarding the rescue of the reprogramming phenotype by the E255K mutant. A recent study suggested that the E255K MENIN mutant almost completely lacks the interaction capability with MLL1 while preserving the ability to interact with JUND to a large extent (Dreijerink et al., 2022). This suggests that there is an additional barrier MENIN imposes in addition to the one it imposes in complex with MLL1. In fact, this is in line with our results showing that there is a much greater increase in the reprogramming efficiency when the cells are knocked out for MEN1 instead of using the inhibitor VTP. While it is not clear that this rescue is due to the preserved interaction with JUND, it certainly warrants further investigation. I believe that the most conclusive way to test this idea is by utilizing a proteolysis targeting chimera (PROTAC) that can successfully and selectively degrade MENIN protein. To my knowledge, there is currently not any PROTAC for MENIN degradation. It should be tested and compared with VTP in the context of reprogramming. Observing a high efficiency with a transient degrader treatment will make reprogramming of human fibroblasts to pluripotency much easier.

Recently, Li et al. showed that MENIN is a reader of H3K79me2 (Lin et al., 2023). In this paper, they had to develop a new method to identify the readers of H3K79me2 where they utilized a nucleosome-based crosslinking-assisted and stable isotope labeling by/with amino acids in cell culture (SILAC)-based protein identification (CLASPI). They found that menin was the only protein that was significantly enriched by the H3K79me2 nucleosome probe (Lin et al., 2023). Since it has already been well-established that inhibiting the only writer of H3K79 methylation, DOT1L, increases the reprogramming efficiency (Onder et al., 2012), we hypothesized that MENIN as a barrier might be working via utilizing its interaction with H3K79me2. We have observed combining MEN1 KO and inhibition in addition to DOT1L inhibitors does not have an additive effect which suggests that they might be working, at least partly, via similar mechanisms. We also know that, in the leukemia context, MENIN inhibition leads to downregulation of

DOT1L expression. While we haven't tested whether this phenomenon is also present in healthy fibroblast cells, it will be worth investigating to see if it is.

Since the initial discovery of reprogramming, the aim in the field was to describe a way to induce pluripotency using only chemicals without overexpressing exogenous genes (Guan et al., 2022). While this has been achieved in mice for a while now, studies that described the chemical induction of pluripotency has come out recently (Guan et al., 2022; Hou et al., 2013). While there are only two papers from the same group published regarding this (Guan et al., 2022; Liuyang et al., 2023), both of these papers utilize the MLL1-MENIN inhibitor, VTP50469. This highlights the fact that the MLL1-MENIN complex imposes a major barrier in somatic cell reprogramming. Considering that our results showed knocking out *MEN1* leads to a superior increase in reprogramming efficiency compared to the inhibitor treatment, it is possible that chemical reprogramming will probably benefit from using a MENIN degrader.

In their 2016 paper, Zhang et al. reported that inhibition or depletion of MLL1 leads to the acquisition of naive pluripotent state in mice. They hypothesized that MLL1 maintains the differentiation/commitment related transcripts and therefore, its inhibition might be leading to the activation of the ground state of pluripotency. They showed that using an MLL1/WDR5 inhibitor leads to the upregulation of the key naive pluripotency markers in an indirect manner (Zhang et al., 2016). These results raise the possibility that MENIN/MLL inhibition might be leading to a similar change. We hypothesize that MENIN acts as a repressor of pluripotency by maintaining the expression of several commitment related genes. Due to the extensive rewiring in the transcription after the inhibition and deletion, both fibroblasts and primed PSCs become more amenable to acquire more less mature identities. In the context of reprogramming, fibroblasts become iPSCs at dramatic speed and efficiency in the absence/inhibition of MENIN. In the context of naive conversion, primed cells go through a more extensive epigenetic resetting in the presence of MENIN/MLL inhibition. It will be interesting to investigate MENIN binding to the chromatin in different cell states, fibroblasts, primed PSCs and naive PSCs. Chromatin Immunoprecipitation (ChIP) sequencing for MENIN targets in these cell types will likely yield the necessary results leading to deciphering the actual mechanism of this enhanced state of "reprogrammability".

Moreover, our RNA-sequencing results showed that, both in MEN1 depletion and inhibiton, a large set of pluripotency-related genes were upregulated under post-OSKM

conditions. This group of genes included pluripotency genes that are usually expressed in the late stages of reprogramming such as NANOG, SALL4 and DNMT3B (Buganim et al., 2013). Interestingly, I observed that MEN1 depletion led to upregulation of 7 pluripotency related genes which include CDH3, a surface marker expressed in successfully reprogrammed iPSCs, under pre-OSKM conditions (Pomeroy et al., 2016). This suggests that MENIN imposes repressive functions on the pluripotency circuitry. Therefore, removing MENIN activity leads to derepression of the pluripotency genes.

Most recently, utilizing naive pluripotent stem cells has gained popularity due to their ability to be used to create embryo models of human development. The highly plastic nature of these cells make them suitable for generating tissues that are present only during the very early stages of development (Kagawa et al., 2022; Oldak et al., 2023; Tarazi et al., 2022). However, the major hurdle in the field currently is the long-term culture and maintenance of these cells. The utilization of the cells in this naive state requires the use of MEK/ERK inhibitors which leads to loss of imprinting after prolonged passaging (Oldak et al., 2023). In addition to these problems, it is also necessary to improve the current media culture conditions. While there is a lot of similarities between pre-implantation embryo and naive cells generated in vitro, there are still a number differences that differentiate the two (Bayerl et al., 2021). Supplementation of VTP50469 into the naive culture conditions leads to a better resetting of the primed state, likely awakening a more plastic ground state. Therefore, adoption of VTP50469 into the currently existing naive PSC protocols would likely result in improved efficiency of better embryo models. This additional supplementation would likely enable the use of reduced concentrations for MEK/ERK inhibition. This, in return, might make naive PSC culture more amenable for long term passaging, enabling the wider use of naive PSCs in developing embryo models. We observed that long term inhibition of MLL1-MENIN complex is feasible for naïve PSC culture for at least 10 passages. This makes the addition of VTP50469 a feasible approach for boosting the naive features of PSCs.

A key feature of naive PSC culture in both mouse and human is the presence of a small population of cells that resemble a much earlier time point in development, the 8-cell stage (Mazid et al., 2022; Taubenschmid-Stowers et al., 2022). Interestingly, the naive cells in culture transiently become 8-cell like cells (8CLC). However, the percentage of these 8CLCs is very low at any given time (Taubenschmid-Stowers et al., 2022). Interestingly, we observed that an 8CLC marker, ARGFX, is expressed at much

greater levels when the MLL1-MENIN complex is inhibited during naive conversion. Since MENIN is expressed at the very early stages of development, it might be imposing another barrier for the acquisition of an 8-cell like cell state. Recently, several groups described methods for generating human 8-cell-like cells in vitro from primed PSCs (Mazid et al., 2022; Yu et al., 2022). These approaches involve the use of different chemical inhibitor cocktails. It will be worth investigating to test if the additional supplementation of VTP50469 would lead to easier acquisition of the 8CLC state.

BIBLIOGRAPHY

Arabacı, D. H., Terzioğlu, G., Bayırbaşı, B., & Önder, T. T. (2021). Going up the hill: Chromatin-based barriers to epigenetic reprogramming. *The FEBS Journal*, *288*(16), 4798–4811. https://doi.org/10.1111/febs.15628

Aztekin, C. (n.d.). *CRISPR-Cas9 based Investigation of Chromatin Modifiers in Human Somatic Cell Reprogramming*.

Bayerl, J., Ayyash, M., Shani, T., Manor, Y. S., Gafni, O., Massarwa, R., Kalma, Y., Aguilera-Castrejon, A., Zerbib, M., Amir, H., Sheban, D., Geula, S., Mor, N., Weinberger, L., Naveh Tassa, S., Krupalnik, V., Oldak, B., Livnat, N., Tarazi, S., … Hanna, J. H. (2021). Principles of signaling pathway modulation for enhancing human naive pluripotency induction. *Cell Stem Cell*, *28*(9), 1549-1565.e12. https://doi.org/10.1016/j.stem.2021.04.001

Bertolino, P., Radovanovic, I., Casse, H., Aguzzi, A., Wang, Z.-Q., & Zhang, C.-X. (2003). Genetic ablation of the tumor suppressor menin causes lethality at mid-gestation with defects in multiple organs. *Mechanisms of Development*, *120*(5), 549–560. https://doi.org/10.1016/S0925-4773(03)00039-X

Blobel, G. A., Kadauke, S., Wang, E., Lau, A. W., Zuber, J., Chou, M. M., & Vakoc, C. R. (2009). A Reconfigured Pattern of MLL Occupancy within Mitotic Chromatin Promotes Rapid Transcriptional Reactivation Following Mitotic Exit. *Molecular Cell*, *36*(6), 970–983. https://doi.org/10.1016/j.molcel.2009.12.001

Borkent, M., Bennett, B. D., Lackford, B., Bar-Nur, O., Brumbaugh, J., Wang, L., Du, Y., Fargo, D. C., Apostolou, E., Cheloufi, S., Maherali, N., Elledge, S. J., Hu, G., & Hochedlinger, K. (2016). A Serial shRNA Screen for Roadblocks to Reprogramming Identifies the Protein Modifier SUMO2. *Stem Cell Reports*, *6*(5), 704–716. https://doi.org/10.1016/j.stemcr.2016.02.004

Buganim, Y., Faddah, D. A., & Jaenisch, R. (2013). Mechanisms and models of somatic cell reprogramming. *Nature Reviews Genetics*, *14*(6), 427–439. https://doi.org/10.1038/nrg3473

Cacchiarelli, D., Trapnell, C., Ziller, M. J., Soumillon, M., Cesana, M., Karnik, R., Donaghey, J., Smith, Z. D., Ratanasirintrawoot, S., Zhang, X., Ho Sui, S. J., Wu, Z., Akopian, V., Gifford, C. A., Doench, J., Rinn, J. L., Daley, G. Q., Meissner, A., Lander, E. S., & Mikkelsen, T. S. (2015). Integrative Analyses of Human Reprogramming

Reveal Dynamic Nature of Induced Pluripotency. *Cell*, *162*(2), 412–424. https://doi.org/10.1016/j.cell.2015.06.016

Canaff, L., Vanbellinghen, J.-F., Kanazawa, I., Kwak, H., Garfield, N., Vautour, L., & Hendy, G. N. (2012). Menin Missense Mutants Encoded by the MEN1 Gene that Are Targeted to the Proteasome: Restoration of Expression and Activity by CHIP siRNA. *The Journal of Clinical Endocrinology & Metabolism*, *97*(2), E282–E291. https://doi.org/10.1210/jc.2011-0241

Çimen, D. U. (n.d.). *Determining the effects of DOT1L interacting proteins on cellular reprogramming*.

Cossec, J.-C., Theurillat, I., Chica, C., Búa Aguín, S., Gaume, X., Andrieux, A., Iturbide, A., Jouvion, G., Li, H., Bossis, G., Seeler, J.-S., Torres-Padilla, M.-E., & Dejean, A. (2018). SUMO Safeguards Somatic and Pluripotent Cell Identities by Enforcing Distinct Chromatin States. *Cell Stem Cell*, *23*(5), 742-757.e8. https://doi.org/10.1016/j.stem.2018.10.001

Dreijerink, K. M. A., Ozyerli-Goknar, E., Koidl, S., Van Der Lelij, E. J., Van Den Heuvel, P., Kooijman, J. J., Biniossek, M. L., Rodenburg, K. W., Nizamuddin, S., & Timmers, H. T. M. (2022). Multi-omics analyses of MEN1 missense mutations identify disruption of menin–MLL and menin–JunD interactions as critical requirements for molecular pathogenicity. *Epigenetics & Chromatin*, *15*(1), 29. https://doi.org/10.1186/s13072-022-00461-8

Ebrahimi, A., Sevinç, K., Gürhan Sevinç, G., Cribbs, A. P., Philpott, M., Uyulur, F., Morova, T., Dunford, J. E., Göklemez, S., Arı, Ş., Oppermann, U., & Önder, T. T. (2019). Bromodomain inhibition of the coactivators CBP/EP300 facilitate cellular reprogramming. *Nature Chemical Biology*, *15*(5), 519–528. https://doi.org/10.1038/s41589-019-0264-z

Gao, Y., Chen, J., Li, K., Wu, T., Huang, B., Liu, W., Kou, X., Zhang, Y., Huang, H., Jiang, Y., Yao, C., Liu, X., Lu, Z., Xu, Z., Kang, L., Chen, J., Wang, H., Cai, T., & Gao, S. (2013). Replacement of Oct4 by Tet1 during iPSC Induction Reveals an Important Role of DNA Methylation and Hydroxymethylation in Reprogramming. *Cell Stem Cell*, *12*(4), 453–469. https://doi.org/10.1016/j.stem.2013.02.005

Guan, J., Wang, G., Wang, J., Zhang, Z., Fu, Y., Cheng, L., Meng, G., Lyu, Y., Zhu, J., Li, Y., Wang, Y., Liuyang, S., Liu, B., Yang, Z., He, H., Zhong, X., Chen, Q., Zhang, X., Sun, S., … Deng, H. (2022). Chemical reprogramming of human somatic

cells to pluripotent stem cells. *Nature*, *605*(7909), 325–331. https://doi.org/10.1038/s41586-022-04593-5

Guo, G., Von Meyenn, F., Rostovskaya, M., Clarke, J., Dietmann, S., Baker, D., Sahakyan, A., Myers, S., Bertone, P., Reik, W., Plath, K., & Smith, A. (2017). Epigenetic resetting of human pluripotency. *Development*, *144*(15), 2748–2763. https://doi.org/10.1242/dev.146811

Guo, X., Liu, Q., Wang, G., Zhu, S., Gao, L., Hong, W., Chen, Y., Wu, M., Liu, H., Jiang, C., & Kang, J. (2013). MicroRNA-29b is a novel mediator of Sox2 function in the regulation of somatic cell reprogramming. *Cell Research*, *23*(1), 142–156. https://doi.org/10.1038/cr.2012.180

Gurdon, J. B., Elsdale, T. R., & Fischberg, M. (1958). Sexually Mature Individuals of Xenopus laevis from the Transplantation of Single Somatic Nuclei. *Nature*, *182*(4627), 64–65. https://doi.org/10.1038/182064a0

Hou, P., Li, Y., Zhang, X., Liu, C., Guan, J., Li, H., Zhao, T., Ye, J., Yang, W., Liu, K., Ge, J., Xu, J., Zhang, Q., Zhao, Y., & Deng, H. (2013). Pluripotent Stem Cells Induced from Mouse Somatic Cells by Small-Molecule Compounds. *Science*, *341*(6146), 651–654. https://doi.org/10.1126/science.1239278

Hu, X., Zhang, L., Mao, S.-Q., Li, Z., Chen, J., Zhang, R.-R., Wu, H.-P., Gao, J., Guo, F., Liu, W., Xu, G.-F., Dai, H.-Q., Shi, Y. G., Li, X., Hu, B., Tang, F., Pei, D., & Xu, G.-L. (2014). Tet and TDG Mediate DNA Demethylation Essential for Mesenchymal-to-Epithelial Transition in Somatic Cell Reprogramming. *Cell Stem Cell*, *14*(4), 512–522. https://doi.org/10.1016/j.stem.2014.01.001

Huangfu, D., Maehr, R., Guo, W., Eijkelenboom, A., Snitow, M., Chen, A. E., & Melton, D. A. (2008). Induction of pluripotent stem cells by defined factors is greatly improved by small-molecule compounds. *Nature Biotechnology*, *26*(7), 795–797. https://doi.org/10.1038/nbt1418

Kaemena, D. F., Yoshihara, M., Beniazza, M., Ashmore, J., Zhao, S., Bertenstam, M., Olariu, V., Katayama, S., Okita, K., Tomlinson, S. R., Yusa, K., & Kaji, K. (2023). B1 SINE-binding ZFP266 impedes mouse iPSC generation through suppression of chromatin opening mediated by reprogramming factors. *Nature Communications*, *14*(1), 488. https://doi.org/10.1038/s41467-023-36097-9

Kagawa, H., Javali, A., Khoei, H. H., Sommer, T. M., Sestini, G., Novatchkova, M., Scholte Op Reimer, Y., Castel, G., Bruneau, A., Maenhoudt, N., Lammers, J.,

Loubersac, S., Freour, T., Vankelecom, H., David, L., & Rivron, N. (2022). Human blastoids model blastocyst development and implantation. *Nature*, *601*(7894), 600–605. https://doi.org/10.1038/s41586-021-04267-8

Katona, B. W., Glynn, R. A., Hojnacki, T. A., & Hua, X. (2019). Menin: Expanding and dichotomous roles in cancer. *Oncoscience*, *6*(9–10), 368–370. https://doi.org/10.18632/oncoscience.485

Koche, R. P., Smith, Z. D., Adli, M., Gu, H., Ku, M., Gnirke, A., Bernstein, B. E., & Meissner, A. (2011). Reprogramming Factor Expression Initiates Widespread Targeted Chromatin Remodeling. *Cell Stem Cell*, *8*(1), 96–105. https://doi.org/10.1016/j.stem.2010.12.001

Kolundzic, E., Ofenbauer, A., Bulut, S. I., Uyar, B., Baytek, G., Sommermeier, A., Seelk, S., He, M., Hirsekorn, A., Vucicevic, D., Akalin, A., Diecke, S., Lacadie, S. A., & Tursun, B. (2018). FACT Sets a Barrier for Cell Fate Reprogramming in Caenorhabditis elegans and Human Cells. *Developmental Cell*, *46*(5), 611-626.e12. https://doi.org/10.1016/j.devcel.2018.07.006

Krivtsov, A. V., & Armstrong, S. A. (2007). MLL translocations, histone modifications and leukaemia stem-cell development. *Nature Reviews Cancer*, *7*(11), 823–833. https://doi.org/10.1038/nrc2253

Leung, C. Y., & Zernicka-Goetz, M. (2015). Mapping the journey from totipotency to lineage specification in the mouse embryo. *Current Opinion in Genetics & Development*, *34*, 71–76. https://doi.org/10.1016/j.gde.2015.08.002

Li, Z., & Rana, T. M. (2012). A kinase inhibitor screen identifies small-molecule enhancers of reprogramming and iPS cell generation. *Nature Communications*, *3*(1), 1085. https://doi.org/10.1038/ncomms2059

Lin, J., Wu, Y., Tian, G., Yu, D., Yang, E., Lam, W. H., Liu, Z., Jing, Y., Dang, S., Bao, X., Wong, J. W. H., Zhai, Y., & Li, X. D. (2023). Menin “reads” H3K79me2 mark in a nucleosomal context. *Science*, *379*(6633), 717–723. https://doi.org/10.1126/science.adc9318

Liuyang, S., Wang, G., Wang, Y., He, H., Lyu, Y., Cheng, L., Yang, Z., Guan, J., Fu, Y., Zhu, J., Zhong, X., Sun, S., Li, C., Wang, J., & Deng, H. (2023). Highly efficient and rapid generation of human pluripotent stem cells by chemical reprogramming. *Cell Stem Cell*, *30*(4), 450-459.e9. https://doi.org/10.1016/j.stem.2023.02.008

Lo, B., & Parham, L. (2009). Ethical Issues in Stem Cell Research. *Endocrine Reviews*, *30*(3), 204–213. https://doi.org/10.1210/er.2008-0031

Matkar, S., Thiel, A., & Hua, X. (2013). Menin: A scaffold protein that controls gene expression and cell signaling. *Trends in Biochemical Sciences*, *38*(8), 394–402. https://doi.org/10.1016/j.tibs.2013.05.005

Mazid, Md. A., Ward, C., Luo, Z., Liu, C., Li, Y., Lai, Y., Wu, L., Li, J., Jia, W., Jiang, Y., Liu, H., Fu, L., Yang, Y., Ibañez, D. P., Lai, J., Wei, X., An, J., Guo, P., Yuan, Y., … Esteban, M. A. (2022). Rolling back human pluripotent stem cells to an eight-cell embryo-like stage. *Nature*, *605*(7909), 315–324. https://doi.org/10.1038/s41586-022-04625-0

Michlits, G., Hubmann, M., Wu, S.-H., Vainorius, G., Budusan, E., Zhuk, S., Burkard, T. R., Novatchkova, M., Aichinger, M., Lu, Y., Reece-Hoyes, J., Nitsch, R., Schramek, D., Hoepfner, D., & Elling, U. (2017). CRISPR-UMI: Single-cell lineage tracing of pooled CRISPR–Cas9 screens. *Nature Methods*, *14*(12), 1191–1197. https://doi.org/10.1038/nmeth.4466

Mikkelsen, T. S., Hanna, J., Zhang, X., Ku, M., Wernig, M., Schorderet, P., Bernstein, B. E., Jaenisch, R., Lander, E. S., & Meissner, A. (2008). Dissecting direct reprogramming through integrative genomic analysis. *Nature*, *454*(7200), 49–55. https://doi.org/10.1038/nature07056

Miles, D. C., De Vries, N. A., Gisler, S., Lieftink, C., Akhtar, W., Gogola, E., Pawlitzky, I., Hulsman, D., Tanger, E., Koppens, M., Beijersbergen, R. L., & Van Lohuizen, M. (2017). TRIM28 Is an Epigenetic Barrier to Induced Pluripotent Stem Cell Reprogramming. *Stem Cells*, *35*(1), 147–157. https://doi.org/10.1002/stem.2453

Milne, T. A. (2017). Mouse models of MLL leukemia: Recapitulating the human disease. *Blood*, *129*(16), 2217–2223. https://doi.org/10.1182/blood-2016-10-691428

Oldak, B., Wildschutz, E., Bondarenko, V., Aguilera-Castrejon, A., Zhao, C., Tarazi, S., Comar, M.-Y., Ashouokhi, S., Lokshtanov, D., Roncato, F., Viukov, S., Ariel, E., Rose, M., Livnat, N., Shani, T., Joubran, C., Cohen, R., Addadi, Y., Kedmi, M., … Hanna, J. H. (2023). *Transgene-Free Ex Utero Derivation of A Human Post-Implantation Embryo Model Solely from Genetically Unmodified Naïve PSCs* [Preprint]. Developmental Biology. https://doi.org/10.1101/2023.06.14.544922

Onder, T. T., Kara, N., Cherry, A., Sinha, A. U., Zhu, N., Bernt, K. M., Cahan, P., Mancarci, B. O., Unternaehrer, J., Gupta, P. B., Lander, E. S., Armstrong, S. A., &

Daley, G. Q. (2012). Chromatin-modifying enzymes as modulators of reprogramming. *Nature*, *483*(7391), 598–602. https://doi.org/10.1038/nature10953

Osnato, A., Brown, S., Krueger, C., Andrews, S., Collier, A. J., Nakanoh, S., Quiroga Londoño, M., Wesley, B. T., Muraro, D., Brumm, A. S., Niakan, K. K., Vallier, L., Ortmann, D., & Rugg-Gunn, P. J. (2021). TGFβ signalling is required to maintain pluripotency of human naïve pluripotent stem cells. *ELife*, *10*, e67259. https://doi.org/10.7554/eLife.67259

Pastor, W. A., Chen, D., Liu, W., Kim, R., Sahakyan, A., Lukianchikov, A., Plath, K., Jacobsen, S. E., & Clark, A. T. (2016). Naive Human Pluripotent Cells Feature a Methylation Landscape Devoid of Blastocyst or Germline Memory. *Cell Stem Cell*, *18*(3), 323–329. https://doi.org/10.1016/j.stem.2016.01.019

Pfaff, N., Liebhaber, S., Möbus, S., Beh-Pajooh, A., Fiedler, J., Pfanne, A., Schambach, A., Thum, T., Cantz, T., & Moritz, T. (2017). Inhibition of miRNA-212/132 improves the reprogramming of fibroblasts into induced pluripotent stem cells by de-repressing important epigenetic remodelling factors. *Stem Cell Research*, *20*, 70–75. https://doi.org/10.1016/j.scr.2017.03.003

Pomeroy, J. E., Hough, S. R., Davidson, K. C., Quaas, A. M., Rees, J. A., & Pera, M. F. (2016). Stem Cell Surface Marker Expression Defines Late Stages of Reprogramming to Pluripotency in Human Fibroblasts. *Stem Cells Translational Medicine*, *5*(7), 870–882. https://doi.org/10.5966/sctm.2015-0250

Qin, H., Diaz, A., Blouin, L., Lebbink, R. J., Patena, W., Tanbun, P., LeProust, E. M., McManus, M. T., Song, J. S., & Ramalho-Santos, M. (2014). Systematic Identification of Barriers to Human iPSC Generation. *Cell*, *158*(2), 449–461. https://doi.org/10.1016/j.cell.2014.05.040

Sevinç, K., Sevinç, G. G., Cavga, A. D., Philpott, M., Kelekçi, S., Can, H., Cribbs, A. P., Yıldız, A. B., Yılmaz, A., Ayar, E. S., Arabacı, D. H., Dunford, J. E., Ata, D., Sigua, L. H., Qi, J., Oppermann, U., & Onder, T. T. (2022). BRD9-containing non-canonical BAF complex maintains somatic cell transcriptome and acts as a barrier to human reprogramming. *Stem Cell Reports*, *17*(12), 2629–2642. https://doi.org/10.1016/j.stemcr.2022.10.005

Sridharan, R., Gonzales-Cope, M., Chronis, C., Bonora, G., McKee, R., Huang, C., Patel, S., Lopez, D., Mishra, N., Pellegrini, M., Carey, M., Garcia, B. A., & Plath, K. (2013). Proteomic and genomic approaches reveal critical functions of H3K9

methylation and heterochromatin protein-1γ in reprogramming to pluripotency. *Nature Cell Biology*, *15*(7), 872–882. https://doi.org/10.1038/ncb2768

Swijnenburg, R.-J., Schrepfer, S., Govaert, J. A., Cao, F., Ransohoff, K., Sheikh, A. Y., Haddad, M., Connolly, A. J., Davis, M. M., Robbins, R. C., & Wu, J. C. (2008). Immunosuppressive therapy mitigates immunological rejection of human embryonic stem cell xenografts. *Proceedings of the National Academy of Sciences*, *105*(35), 12991–12996. https://doi.org/10.1073/pnas.0805802105

Takahashi, K., & Yamanaka, S. (2006). Induction of Pluripotent Stem Cells from Mouse Embryonic and Adult Fibroblast Cultures by Defined Factors. *Cell*, *126*(4), 663–676. https://doi.org/10.1016/j.cell.2006.07.024

Takashima, Y., Guo, G., Loos, R., Nichols, J., Ficz, G., Krueger, F., Oxley, D., Santos, F., Clarke, J., Mansfield, W., Reik, W., Bertone, P., & Smith, A. (2014). Resetting Transcription Factor Control Circuitry toward Ground-State Pluripotency in Human. *Cell*, *158*(6), 1254–1269. https://doi.org/10.1016/j.cell.2014.08.029

Tarazi, S., Aguilera-Castrejon, A., Joubran, C., Ghanem, N., Ashouokhi, S., Roncato, F., Wildschutz, E., Haddad, M., Oldak, B., Gomez-Cesar, E., Livnat, N., Viukov, S., Lokshtanov, D., Naveh-Tassa, S., Rose, M., Hanna, S., Raanan, C., Brenner, O., Kedmi, M., … Hanna, J. H. (2022). Post-gastrulation synthetic embryos generated ex utero from mouse naive ESCs. *Cell*, *185*(18), 3290-3306.e25. https://doi.org/10.1016/j.cell.2022.07.028

Taubenschmid-Stowers, J., Rostovskaya, M., Santos, F., Ljung, S., Argelaguet, R., Krueger, F., Nichols, J., & Reik, W. (2022). 8C-like cells capture the human zygotic genome activation program in vitro. *Cell Stem Cell*, *29*(3), 449-459.e6. https://doi.org/10.1016/j.stem.2022.01.014

Theunissen, T. W., Powell, B. E., Wang, H., Mitalipova, M., Faddah, D. A., Reddy, J., Fan, Z. P., Maetzel, D., Ganz, K., Shi, L., Lungjangwa, T., Imsoonthornruksa, S., Stelzer, Y., Rangarajan, S., D'Alessio, A., Zhang, J., Gao, Q., Dawlaty, M. M., Young, R. A., … Jaenisch, R. (2014). Systematic Identification of Culture Conditions for Induction and Maintenance of Naive Human Pluripotency. *Cell Stem Cell*, *15*(4), 471–487. https://doi.org/10.1016/j.stem.2014.07.002

Toh, C.-X. D., Chan, J.-W., Chong, Z.-S., Wang, H. F., Guo, H. C., Satapathy, S., Ma, D., Goh, G. Y. L., Khattar, E., Yang, L., Tergaonkar, V., Chang, Y.-T., Collins, J. J., Daley, G. Q., Wee, K. B., Farran, C. A. E., Li, H., Lim, Y.-P., Bard, F. A., & Loh,

Y.-H. (2016). RNAi Reveals Phase-Specific Global Regulators of Human Somatic Cell Reprogramming. *Cell Reports*, *15*(12), 2597–2607. https://doi.org/10.1016/j.celrep.2016.05.049

Waddington, C. H. (2014). *The Strategy of the Genes* (0 ed.). Routledge. https://doi.org/10.4324/9781315765471

Yagi, H., Deguchi, K., Aono, A., Tani, Y., Kishimoto, T., & Komori, T. (1998). Growth disturbance in fetal liver hematopoiesis of Mll-mutant mice. *Blood*, *92*(1), 108–117.

Yang, C.-S., Chang, K.-Y., & Rana, T. M. (2014). Genome-wide Functional Analysis Reveals Factors Needed at the Transition Steps of Induced Reprogramming. *Cell Reports*, *8*(2), 327–337. https://doi.org/10.1016/j.celrep.2014.07.002

Yokoyama, A., & Cleary, M. L. (2008). Menin Critically Links MLL Proteins with LEDGF on Cancer-Associated Target Genes. *Cancer Cell*, *14*(1), 36–46. https://doi.org/10.1016/j.ccr.2008.05.003

Yokoyama, A., Somervaille, T. C. P., Smith, K. S., Rozenblatt-Rosen, O., Meyerson, M., & Cleary, M. L. (2005). The Menin Tumor Suppressor Protein Is an Essential Oncogenic Cofactor for MLL-Associated Leukemogenesis. *Cell*, *123*(2), 207–218. https://doi.org/10.1016/j.cell.2005.09.025

Yu, X., Liang, S., Chen, M., Yu, H., Li, R., Qu, Y., Kong, X., Guo, R., Zheng, R., Izsvák, Z., Sun, C., Yang, M., & Wang, J. (2022). Recapitulating early human development with 8C-like cells. *Cell Reports*, *39*(12), 110994. https://doi.org/10.1016/j.celrep.2022.110994

Zernicka-Goetz, M., & Hadjantonakis, A.-K. (2014). From pluripotency to differentiation: Laying foundations for the body pattern in the mouse embryo. *Philosophical Transactions of the Royal Society B: Biological Sciences*, *369*(1657), 20130535. https://doi.org/10.1098/rstb.2013.0535

Zhang, H., Gayen, S., Xiong, J., Zhou, B., Shanmugam, A. K., Sun, Y., Karatas, H., Liu, L., Rao, R. C., Wang, S., Nesvizhskii, A. I., Kalantry, S., & Dou, Y. (2016). MLL1 Inhibition Reprograms Epiblast Stem Cells to Naive Pluripotency. *Cell Stem Cell*, *18*(4), 481–494. https://doi.org/10.1016/j.stem.2016.02.004

Appendix 1

We have generated blastoids as previously described (Kagawa et al., 2022) using the naive PSCs acquired by converting the WIBR3 OCT4 GFP ESC line using the HENSM conditions supplemented with 1 uM VTP50469. Briefly, the naive cells were detached from the plate using Accutase. Then, the cells were counted. For each well of a 24 well plate Aggrewell 400, 66,000 cells were seeded (55 cells/microwell). The aggregation was performed in the N2B27 base media (50% DMEM/F12, 50% Neurobasal, 1% Glutamax, 1% NEAA, 2-mercaptoethanol (100 uM), bovine serum albumin solution (0.45%), 1% N2, 2% B27). The next day, the media was switched to the PALLY media (N2B27 base media supplemented with 1 uM PD0325921, 1 uM A83-01, 1 uM or 5 uM 1-oleyl lysophosphatidic acid (LPA), hLIF (10 ng/mL), 10 uM Y-27632). After 48 h, the media is switched to LY media (N2B27 base media supplemented with 1 uM or 5 uM and 10 uM Y-27632) (Figure A.1 and Figure A.2).

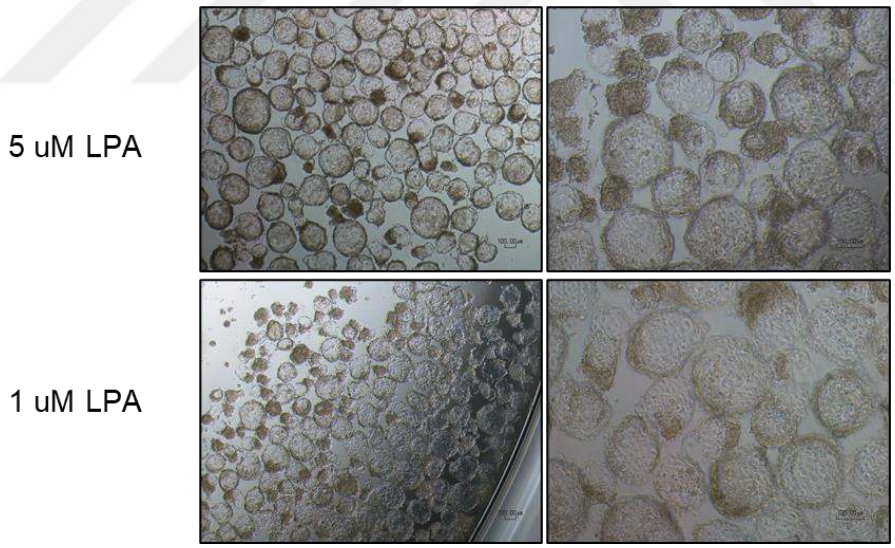

Figure A.1. Blastoids formed using the naive cells acquired with HENSM conditions supplemented with 1 μM VTP50469. 1 μM and 5 μM LPA concentrations were used to generate the blastoids. Scale bars denote 100 μM.

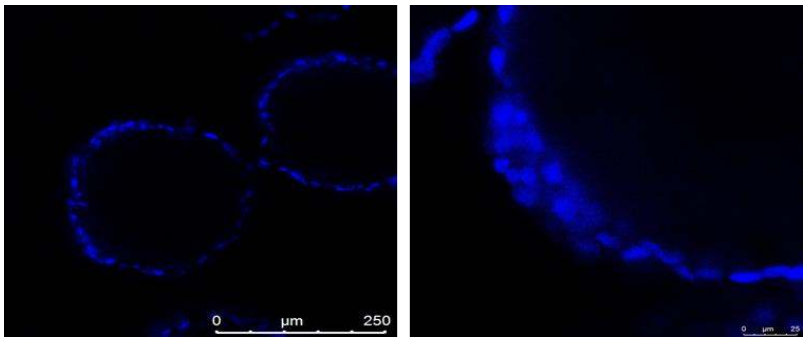

Figure A.2. Blastoids generated with 5 uM LPA stained with DAPI to visualize the nuclei. Scale bars denote 250 uM or 25 uM.

Moreover, I have cloned the MEN1 sequence onto the pLEX 305 backbone containing dTAG sequence, tagging MENIN on the N-terminal and C-terminal with the dTAG protein (Figure A.4). I have generated these plasmids to induce rapid MENIN degradation during reprogramming (Figure A.3). To test this, I overexpressed these plasmids in MEN1 KO fibroblasts. I have shown that 2 hour treatment of the cells overexpressing C-dTAG MEN1 with dTAG-47 compound leads to rapid MENIN degradation (Figure A.5). Additionally, I have observed that this tagged MEN1 plasmid can rescue the MEN1 KO reprogramming phenotype (Figure A.6)

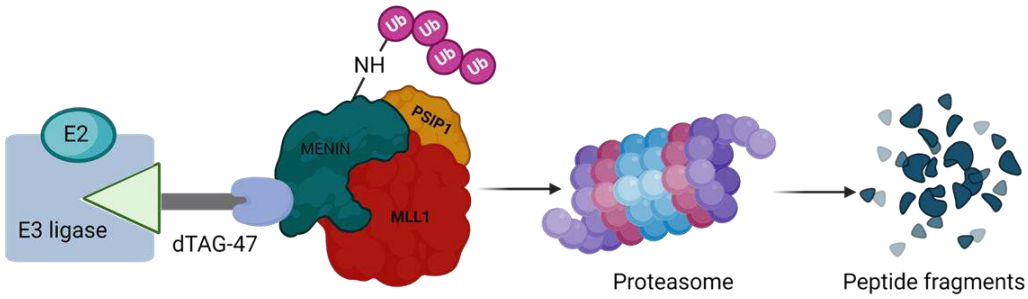

Figure A.3. The schematics of the dTAG MENIN degradation induced by dTAG-47 treatment.

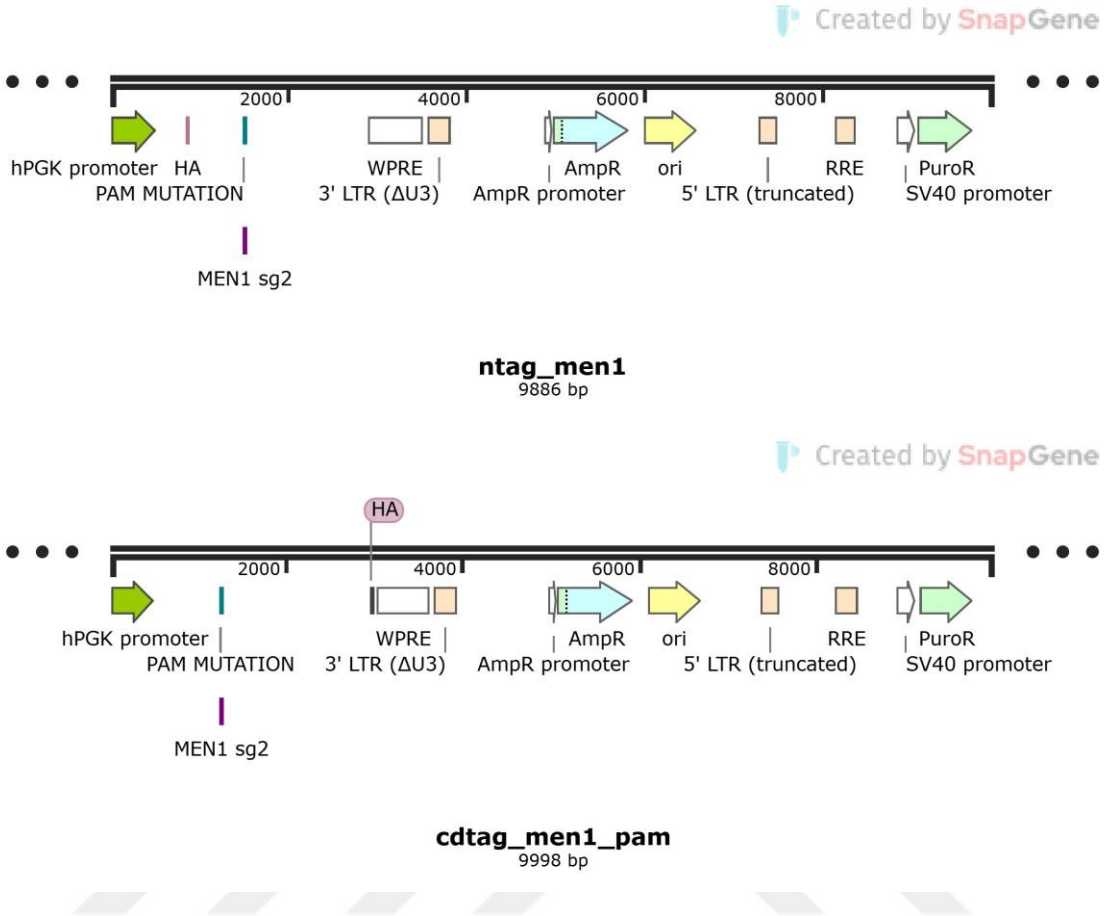

Figure A.4. The plasmid maps of N-dTAG MEN1 and C-dTAG MEN1.

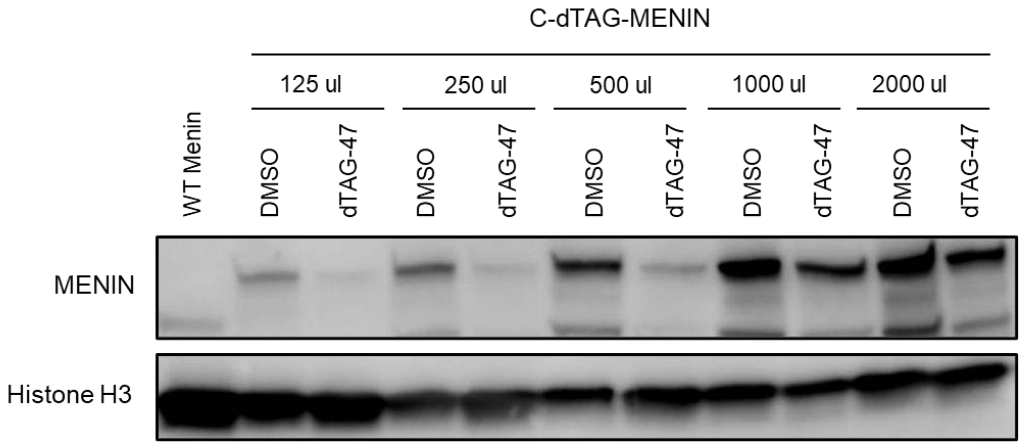

Figure A.5. Degradation of C-dTAG MENIN overexpressed at different levels after 2 hours of treatment with 500 nM dTAG-47.

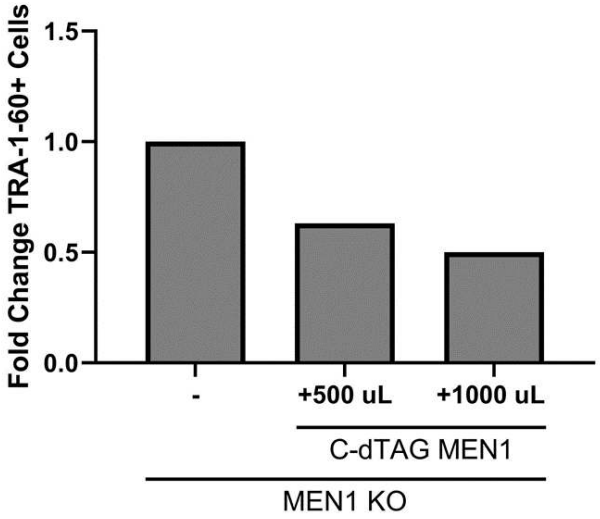

Figure A.6. The fold change in the number of TRA-1-60+ cells on day 6 of reprogramming quantified by flow cytometry analysis. C-dTAG MEN1 was overexpressed in different amounts in *MEN1* knockout fibroblasts.